ADDIS ABABA UNIVERSITY

INSTITUTE OF TECHNOLOGY

Design and Development of *teff* seed broadcaster

by

Abdulhakim Shukurea

a Thesis

Submitted in Partial Fulfillment of the Requirement for The

Master of Science Degree

in

Mechanical Engineering

(Mechanical Design)

Advisor

Dr.-Ing Zewdu Abdi

2012

ACKNOWLEDGEMENT

First and foremost I would like to express my deepest and heartfelt thanks as well as my most sincere appreciation to my research advisor Dr.-Ing Zewdu Abdi for his consistent guidance, critical review and for commenting on the manuscript throughout the course of this research starting from proposal preparation up to the final thesis write up. His readiness in providing assistance and advice greatly helped me to carry out the study.

My deep gratitude and acknowledgements goes to Mr. Girma Moges of Ethiopia Agricultural Research Institute for providing me useful data. My deep gratitude and acknowledgements also goes to Mr. Hailu Luche of Caleb farmers House for providing me important information.

Finally all my heartfelt and deepest appreciation goes to my friend Selamawit Tesfa, my beloved mother, my beloved sisters, brother and friends whose persistent support and encouragement unreserved love and all-rounded assistance which was a substantial input to my inspiration and effort throughout the course of the research work.

ABSTRACT

An analysis of the motion of teff seed particle on a rotating cone shaped disc is conducted and also basic equations of motion derive for a single teff seed particle. The analysis directly applied to the flow of teff seed particle on a spinning disc spreader. Equations of motion are developed for cone shaped disc and pitched type vane spreader. The derived equation of motion form parts of the basis of MATLAB-SIMULINK model simulation for spinning disc spreader with equation of motion through the air (off-disc) model. In MATLAB-SIMULINK simulation, the motion of single teff seed particle is considering with different initial conditions (physical properties of *teff* seed such as moisture content) and also varying different machine parameters (such as cone angle, pitch angle and rotational speed of disc). Different machine parts were designed and the mass flow rate of *teff* seed was calculated. Seed hopper was also designed. Shafts were designed and selecting of material for shaft was done, and checked. Bevel gear was designed and the principal dimension was found. Four bearings were selected and checked for stability under the existing loads.

Table of Contents

LIST OF FIGURES

LIST OF TABLE

NOTATION

Bhn	Brinell hardness number
F_{ce}	Centrifugal forces
F_g	Gravitational forces
F_{co}	Coriolis forces
F_I	Inertial forces
m_p	Mass of particles (*teff*)
μ_v	Coefficient of friction between the vane and the teff
μ_d	Coefficient of friction between the disc and the teff
$\boldsymbol{F_r}$	Radial load
F_a	Axial load
F_A^X	Reaction force in the X-axis at point A
F_A^Y	Reaction force in the Y-axis at point A
F_A^Z	Reaction force in the Z-axis at point A
F_B^Y	Reaction force in the Y-axis at point B
F_B^Z	Reaction force in the Z-axis at point B
F_C^X	Reaction force in the X-axis at point C
F_C^Y	Reaction force in the Y-axis at point C
F_C^Z	Reaction force in the Z-axis at point C
F_D^X	Reaction force in the Y-axis at point D
F_D^Z	Reaction force in the Z-axis at point D
MG_{XY}	Bending moment in the X-Y plane
M_G	Total bending at point G

V_D	Discharge velocity
V_r	Radial velocity
V_t	Tangential velocity
R	Radius of disc
ρ_t	Density of teff seed particle
ρ_A	Density of air
β	Pitch angle
ω	Angular velocity
α	Cone angle
G	Gravitational acceleration
H	Height
A_f	Frontal area
C_D	Drag coefficient
F_D	Drag force
σ_{ut}	Ultimate stresses
σ_e	Equivalent stresses
σ_y	Yield stresses
f_s	Factor of safety
L_D	Life of bearing
W_d	Basic dynamic equivalent radial load
X	Radial load factor

Y	Axial load factor
C_d	Basic dynamic load rating
Cs	Basic static load rating
K	Aerodynamic resistance coefficient
MC	Moisture content
l	slant height
∅	Angle repose
$\dot{m}$	Mass flow rate of teff seed
V	Volume of hopper
D	upper diameter of hopper
d	bottom diameter of hopper

1. Introduction

Teff (Eragrostis *teff* (Zucc) Trotter) originated in Ethiopia, where it is widely cultivated (Seyfu, 1997). Details of its domestication are unknown, but it may predate the introduction of wheat and barley to the region. *Teff* is perhaps descended from the closely related wild Eragrostis pilosa Beauv, which is a tetraploid annual like *teff*, and which has a cosmopolitan distribution. Grain cultivation of *teff* has been confined mainly to Ethiopia and to some extent to the highlands of Eritrea. It is also grown in northern Kenya. Small-scale commercial *teff* production takes place in South Africa, the United States, Canada, Australia, Europe (the Netherlands) and Yemen (Seyfu, 1997). Additionally, Seyfu (1997) commented teff is grown as a forage grass, for instance in South Africa, Morocco, Australia, India and Pakistan. It has been introduced experimentally into other tropical countries, either for its grain or for hay, e.g. in other parts of East Africa and in southern Africa. It is commonly found as an escape from cultivation. The composition of *teff* is similar to that of millet, although it contains generally higher amounts of essential amino acids. The amino acid composition of *teff* is excellent, its lysine content is higher than that of all cereals except rice and oats, it has good mineral content and its straw is nutritious (Seyfu, 1997).

A high cereal yield requires a high field emergence and a uniform development of each plant. To achieve this, there is a requirement for a uniform sowing depth as well as a uniform seed distribution over the area. Both depend on the techniques used for seed placement into the soil.

For about a century, drilling has been the dominant technique for seed placement into the soil. The seed may be deposited by shoe openers, disc openers, or sometimes in the furrows of packer rings.

Broadcast sowing is carried out by simply dropping seed freely onto the soil surface in front of a cultivator. The drawback of broadcasting is its weakness in seed depth and its merits is uniform distribution over the area. Broadcasting as one of the seed sowing methods, in combination with reduced cultivation offers the advantage of being up to four times faster than conventional ploughing and drilling particular value for sowing large hectare of winter cereals (Ball, 1986). Row planting minimizes lodging under good growth conditions and broadcasting minimizes time and production cost.

Seeding in a band having a width of 3 to 4 cm can be accomplished in several ways. In some cases, disc-openers slightly angled to the direction of travel are used to create the necessary furrow width. When soil cultivation and sowing are combined, seed tubes located in the soil flow of the tines can place the seed in a band of this width. For band widths ranging from 8 to 16 cm, special coulters such as wing openers or broad-shoe openers have been developed. Wing openers lift the soil, whereas broad-shoe openers move it sideways within the band width. At the bottom of these openers the seed hits a baffle, which causes *broadcasting* within the coulter space. When the opener spacing across the width of the machine is decreased to fit the band width, broadcasting is achieved over the whole area.

Teff is propagated by seed. There is no seed dormancy and germination is rapid. The 1000-seed of *teff* weight is 300–400 mg in the moisture content range from 5.6% to 29.6% w.b. (Zewdu & Solomon, 2007). *Teff* seeds remain viable for several years provided direct contact with moisture and sunshine is avoided. In Ethiopia centuries-old traditional practices are used in *teff* production. An oxen-drawn plough (‘*maresha*’) is used to till the land, with 2–5 passes made before sowing. Studies indicate that *teff* can be successfully grown under reduced tillage conditions (one ploughing to bring the seeds in contact with the soil) provided non-selective herbicides are used (Seyfu, 1997). To enhance germination and seedling establishment on Vertisols, a firm seedbed is made by trampling with farm animals. Normally farmers sow *teff* by broadcasting on a moist, fine seedbed. A seed rate of 15–30 kg/ha is sufficient, but farmers often use 40–50 kg/ha, because it is difficult to distribute the seed evenly, the viability of farmers’ own seed is reduced, and it helps to suppress weeds at early stages (Seyfu, 1997). The seeds are left uncovered or covered lightly by pulling branches over the field using oxen. *Teff* can also be drilled in rows using adjusted machinery.

Application of planting of *teff* is still performed largely by traditional methods in Ethiopia. Farmers normally use hand-broadcasting method for broadcasting *teff*. In this method, *teff* cannot be uniformly distributed in the field. As a result, low efficiency and high cost are being incurred. To obtain satisfactory crop yield one should plant particular amount of *teff* in a given area uniformly. The principal disadvantage of traditional hand-broadcasting method is the non-uniform distribution of material and thus non-optimal use of resources. Furthermore, it requires

experienced manpower to broadcast. It was expected that spreading of *teff* by mechanical means could be more uniform and achieve high field capacity compared to traditional hand broadcasting. So it is necessary to design spinning disc broadcaster to solve the problem to get uniform mass distribution of *teff* in the field and increasing the yield and also reducing machinery cost it can be also used for fertilizer broadcasting.

The spinner spreader consists of a rotating disc with vanes bolted to the disc surface. *Teff* poured onto the spinner is thrown onto the ground after colliding with the rotating vanes. The main advantages of the spinner spreader are that it has a large spread width, small size, simple and robust construction and is inexpensive to produce.

1.1. Statement of the problem

In general broadcasting of *teff* is done by hand in almost all over Ethiopia this leads to low yields of teff per hectare. The causes among others include.

- Lack of uniform distribution of *teff* in field due to wind, human ability to distribute evenly
- Waste of seed *teff* as the amount hand broadcasted is higher to overcome un even distribution to bring overlapping of *teff* sown
- Requires higher man-days to broadcast

Since *teff* is the staple food of most Ethiopian people, the present production system cannot satisfy the consumers' demand. This is because the farming system that farmers use is backward which is not supported by modern technologies. This means the local people use hand broadcasting system rather than using mechanical seeding method. *Teff* has the lowest in yield of all the cereals grown in the country 9-10qt/ ha (Seyfu, 1997).

As the population increases and the demand of t*eff* rises, the supply is not increasing at the same rate. The price of *teff* is going up. Consumers who have less income could not afford the price of teff. How long this problem goes on? How could this problem be tackled?

When *teff* production is unwise and inefficient, it is not only wastage of resources but also a negative implication on the yield of teff. The growth of *teff* will be challenged due to factor such

as lack of enough space between teff seeds, lack of uniform distribution of seeds, low production.

1.2. General objective

To design and development of *teff* seed broadcaster

1.3. Specific objectives

- To find the different properties of *teff* seeds particles related to broadcasting
- To model and simulate *teff* seed trajectory on the disc and off the disc
- Design and development a spreader type broadcaster

1.4. Methodology

The methods to be employed to achieve the objective of the research are broken down in different phases:

a. Literature review

In addition to the literature survey to be carried out, the following tasks will be done

- Information gathering will be conducted from farmer and
- Minister of agriculture
- Agricultural machine importer, manufactures and research organization

b. Mathematical Modeling and simulating

The necessary concepts will be developed and design of different component as shown below

- Modelling of the forces acting on a *teff* seed on a seed broadcaster
- Studying the particles trajectory with varying design parameters of the spreader
    - Disc rotation speed
    - Feed radius
    - Angle of vanes
    - *Teff* seed property related to broadcasting
    - Cone angle

c. Mechanical parts design

Different parts of spinning disc broadcaster will be analytically design and check their stability under the existing force.

1.5. Significance of the study

The importance of design of *teff* seed broadcaster is to increase production of *teff* through uniform distribution of *teff* seed in the field and also reduce man-day to broadcast, as well saving the seed per hectare to be sown.

1.6. Organization of the thesis

Chapter one describes a general introduction of the Thesis. Chapter two reviews literatures about particles trajectory on disc and off disc. Chapter three presents mathematical modeling of *teff* seed particles on the disc and teff seed particles off the disc. Chapter four presents simulation of *teff* seed on-disc and off-disc. Chapter five presents design of different mechanical parts and selection of parts. Chapter six give a short recommendation and conclusions.

2. Literature review

The performance of spinner spreaders has been widely investigated. Studies have typically focused on analytical models for particle trajectories on and off of the spinner and design of spinner disc for fertilizer. Several experimental studies have also been performed, but these often utilize idealized particles, typically steel ball bearings, or a limited number of granular fertilizer. An excellent summary of many of these studies

Patterson and Reece (1962) investigated the motion of spherical particles on a spinner with a near-center fed neglecting particle bounce off of the spinner vanes. They developed analytical models for on-spinner particle motion and found reasonable agreement between their models and experimental measurements of the radial and total velocities of steel ball bearings leaving the spinner plate as well as the angle between where particles are dropped and where they leave the spinner plate.

Aphale et.al, (2003) conducted experimental and analytical study to investigate particles trajectories on and off spinner spreader. They use sixteen different granular fertilizers the experiment data for on spinner trajectories generally lie between the analytical models for the pure rolling and pure sliding condition using a sliding friction coefficient of 0.5.

Hofstee (1994, 1995) utilized an ultrasonic transducer to determine the velocity and direction of particles leaving a spinner spreader. He found that the friction coefficient between a particle and the spinner plate and vane is a significant variable; however, obtaining representative values for this variable for use in on-spinner models is difficult.

Dintwa et al. (2004a) suggested calibration of the simulation input parameters using a 'landing area', which represents the collective effect of the various particle interactions during movement along the vane and disc. They assumed that the discrepancies between simulation and measured spread patterns were mostly owing to particle interactions. The researchers identified the most important parameters that affected the 'landing area' such as the mass flow rate, the disc radius, the disc rotational speed, the orifice radial dimensions and the vane pitch, and presented calibration curves for the individual parameters. They suggested that the model, which considers particle interaction, improves simulation results and requires fewer calibrations.

Olieslagers et al. (1996) also generalized the models developed by earlier researchers and found large discrepancies between predicted spread pattern and an experimental distribution owing to ignoring particle interactions. For this reason they suggested a corrected method by adjusting the simulation input parameters to fit the experimental data. In addition, they reported that the angular velocity of the disc, the position of the orifice, shape of the orifice opening, and the mass flow have a major influence on the shape and the width of the spread pattern.

Ziauddin and Roy (1997) developed and tested a low cost seed-cum-fertilizer distributor for broadcasting seeds and fertilizer in the field. The materials to be distributed fell down by the gravity from a tank on a fixed metallic platform. A hand-operated rotor distributed the materials uniformly. This simple mechanical device was designed to carry on the shoulder of an operator during operation. The Uniformity Coefficient of Distribution of traditional broadcasting system was about 30% to 43% depending up on the labor skills. But the average uniformity coefficient of distribution of this device was about 82.32%, 80.43% and 85.66% for the fine urea, granular urea and wheat, respectively.

Tajuddin (1989) designed, developed and tested a hand rotary-broadcasting device for broadcasting seeds, fertilizers and granular insecticides in laboratory and field. The uniformity co-efficient of distribution was determined for spreading urea using the broadcasting device and compared with that of the hand broadcasting process. The device's coverage was 1.26 ha/hr in paddy. The unit had a weight of 3.6 kg and cost of US$ 55 and average Uniformity Coefficient of Distribution was 50 % (Tajuddin, 1989)

These previous investigations have showed that how to model the dynamics of particles distributed by a spinner disc spreader and also prepare the necessary information for the design of spreader using particles trajectory.

2.1. Physical properties of *teff* seed

Zewdu and Solomon (2007) investigated that the physical properties of teff seed in the moisture content of 5.6% to 29.6%. The length, width and equivalent-sphere diameter of *teff* seeds increased from 1.01 to 1.27 mm, 0.59 to 0.68 mm and 0.71 to 0.87 mm, respectively.

Zewdu and Solomon (2007) further conducted experiment on *teff* seed and they found that the Sphericity decreased from 0.70 to 0.63 with increase in the moisture content from 5.6% to 21.43% and increased to 0.69 with further increase in moisture content to 29.6% and the thousand mass of *teff* seed increased from 0.257 to 0.421 g with the corresponding increase in moisture content. According to Zewdu and Solomon they found that the bulk and true densities of samples decreased with increase in moisture content .A decrease from 840 to 696 kgm^{-3} and 1361 to 1207 kgm^{-3} was observed for bulk and true densities, respectively, in the moisture content range studied.

Zewdu and Solomon (2007) they conducted experiment on the moisture-dependent properties of *teff* seed and they found that the angle of repose change as the moisture content increase. Arise in moisture content from 5.6% to 29.6% w.b resulted increment of angle of response 23.74^0 to 51.6^0.Angle of repose is the maximum slop at which stack of any losses or fragmented bulk material will stand without sliding (Chelecho, 2003). The coefficients of friction of teff seed was changed from 0.29 to 0.53 on mild steel as moisture content increase from 5.6% to 29.6% respectively (Zewdu and Solomon, 2007).

3. Mathematical modeling

The mathematical modeling analysis of *teff* particle is presented in two sections: particle dynamics on the spinner plate (on disc) and particle dynamics after the particle has left the spinner plate (off-disc). In both of this analysis, it is assumed that particle does not interact with one another and the mode of travel is sliding.

The important design factors of a spinning disc are the disc radius, the feed radius, the pitch angle of the vane and the cone angle of the disc.

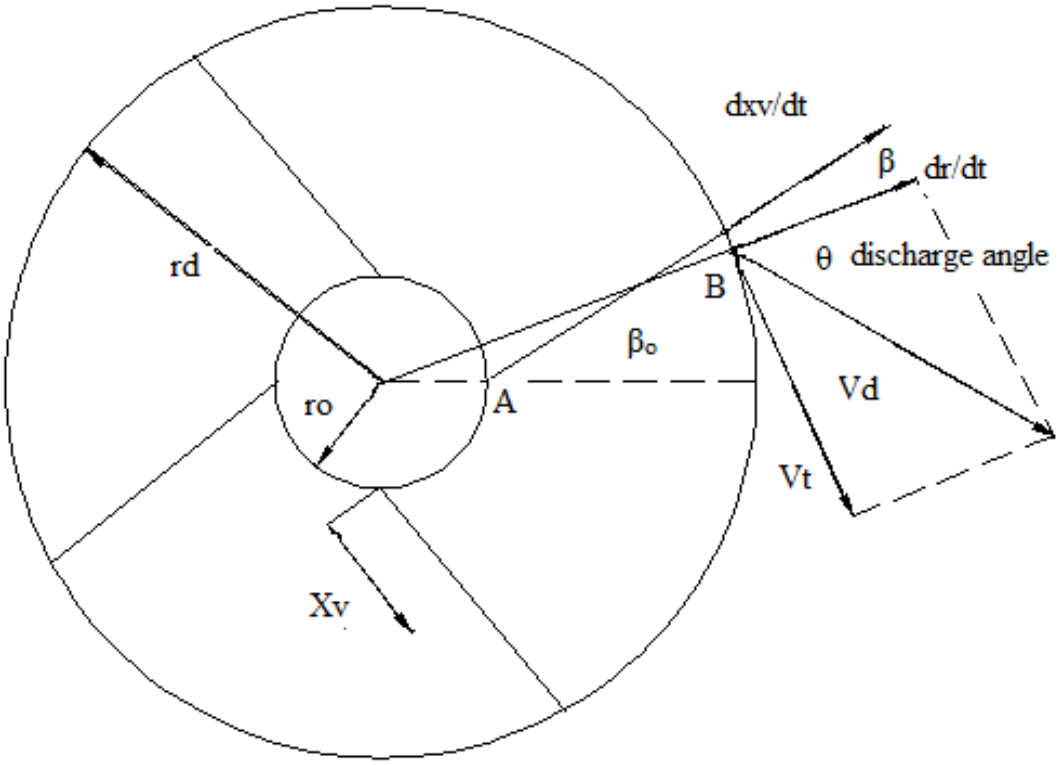

Figure 1: Important disc design parameter

3.1. Equation of teff particle motion on disc

The motion of the particle on the spinning disc can be described by differential equation that can be derived from the force acting on the particle by using D' Alembert's principle .

When analyzing the motion of *teff* seed it is necessary to assume the shape of the vane. The vane can be taken as straight for simplicity and placed on the disc with an angle with respect to the

radial line, if the pitch angle is greater than zero, it is called backward pitched and if the pitch angle is less than zero, it is called forward pitched.

From Fig. 1 we derive the pitch angle to be

$$\beta = \tan^{-1}\left(\frac{r_o \sin\beta_o}{x_v + r_o \cos\beta_o}\right) \qquad \text{(Eq. 3.1)}$$

The above formula shows that the pitch angle for straight radial vane depends on the particle radial position.

From Figure 1 to evaluate the disc radius by using cosine law and take the triangle OAB

$< OBA = \emptyset$

$\emptyset = 180 - \beta_o$

$\cos\emptyset = \cos(180 - \beta_o) = \cos\beta_o$

$OA^2 = OB^2 + AB^2 + 2AB * OB * \cos\beta_o)$

$$r = \sqrt{r_o^2 + x_v^2 + 2r_o x_v \cos(\beta_o)} \qquad \text{(Eq. 3.2)}$$

3.1.1. Centrifugal forces

The centrifugal force always acts on the horizontal plane along a line through the center of rotation and the radial position of the particle. Then the centrifugal force can be resolved in:

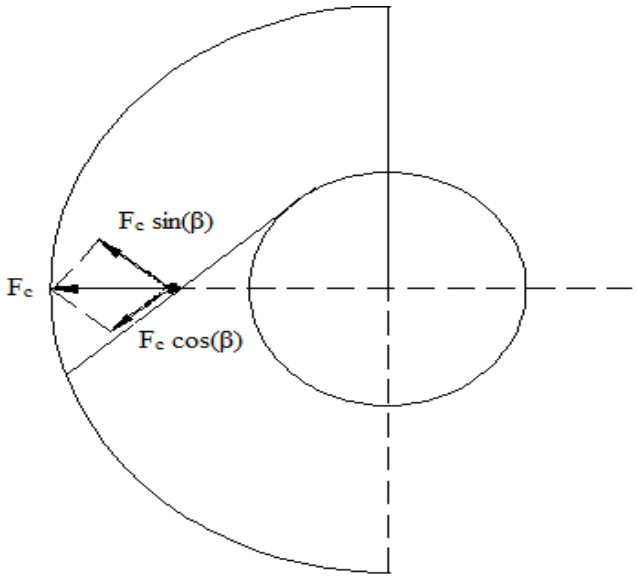

Figure 2: Centrifugal force acting on teff seed particle

$\sum F_{cex} = F_{ce} \cos\alpha \cos\beta$ in the diction of motion (Eq. 3.3)

$\sum F_{cey} = F_{ce} \sin\alpha \cos\beta$ perpendicular to the disc (Eq. 3.4)

$\sum F_{cez} = -F_{ce} \sin\beta$ perpendicular to the vane (Eq. 3.5)

3.1.2. Coriolis force

The Coriolis force always acts in the horizontal plane and is perpendicular to the direction of motion. Only the horizontal component of the velocity along the vane is of relevance.

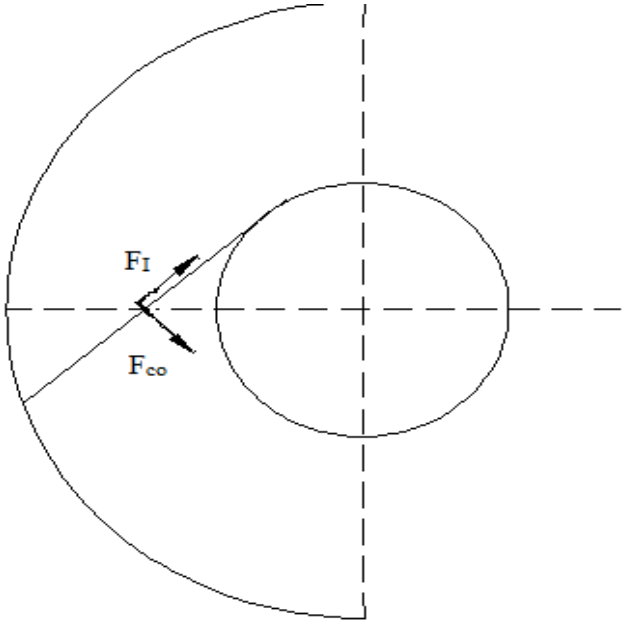

Figure 3: Coriolis force and Mass inertia

$\sum F_{co} = 2m_p \cos\alpha \, w_d \frac{dx_v}{dt}$ Perpendicular to the vane (Eq. 3.6)

3.1.3. Mass inertia

The mass inertia always acts in a line in the direction of motion

$F_I = m_p \frac{d^2x_v}{dt^2}$ (Eq. 3.7)

3.1.4. Gravity

The gravity always acts in the vertical plane along a line in the direction of the center of the earth. Then, the gravity can be resolved in

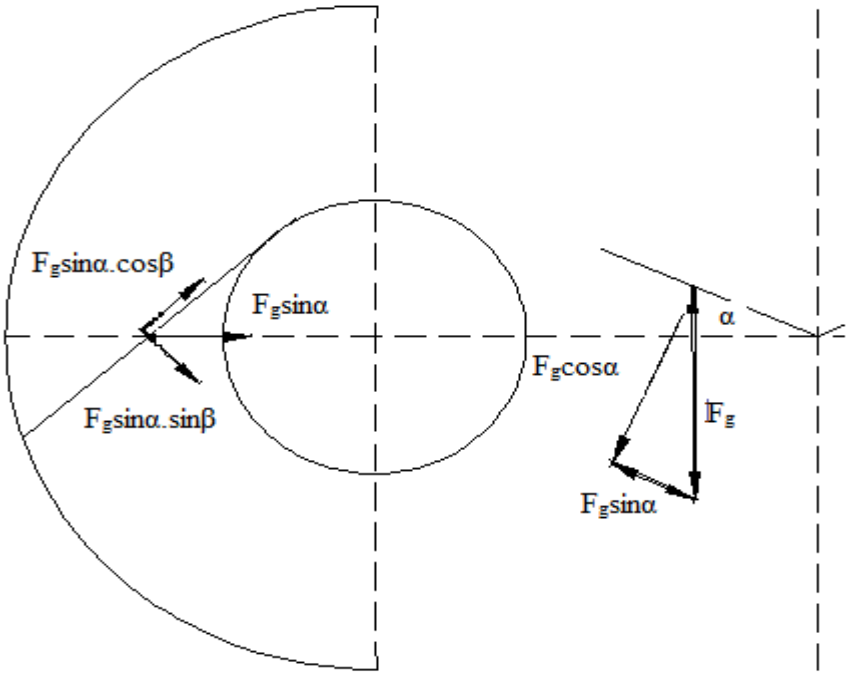

Figure 4: Gravity

$\sum F_{xg} = F_g \sin\alpha \cos\beta$ Direction of motion (Eq. 3.8)

$\sum F_{yg} = F_g \cos\alpha$ Perpendicular to the disc (Eq. 3.9)

$\sum F_{zg} = F_g \sin\alpha \sin\beta$ Perpendicular to the vane (Eq.3.10)

3.1.5. Friction

All forces except mass inertia have at least one component perpendicular to the vane or disc surface and cause friction force acting in the direction opposite to the direction of motion.

Friction force due to centrifugal forces:

$F_{cefd} = -m_p \omega_d^2 r \sin\alpha \cos\beta \, \mu_d$ (Eq.3.11)

$F_{cefv} = -m_p \omega_d^2 r \sin\beta \, \mu_v$ (Eq. 3.12)

Friction force due to Coriolis force

$$F_{cof} = -2\cos\alpha\,\mu_v\omega_d\frac{dx_v}{dt} \quad \text{(Eq. 3.13)}$$

Friction forces due to gravity

$$F_{gfd} = F_g\cos\alpha\,\mu_d \quad \text{(Eq. 3.14)}$$

$$F_{gfv} = F_g\sin\alpha\sin\beta\,\mu_v \quad \text{(Eq. 3.15)}$$

Then the general equation of motion along in pitched line is

$$\sum F_x = m_p\frac{d^2x_v}{dt^2} \quad \text{(Eq. 3.16)}$$

Sub. Eq. 3.3to Eq. 3.16 and rearranging and cancelled out m_p

$$\frac{d^2x_v}{dt^2} + 2\cos\alpha\,\mu_v\omega_d\frac{dx_v}{dt} - (\cos\alpha\cos\beta - \sin\alpha\cos\beta\,\mu_d + \sin\beta\,\mu_v)\omega_d^2 r + (\sin\alpha\cos\beta + \sin\alpha\sin\beta\,\mu_v + \cos\alpha\,\mu_d)g = 0 \quad \text{(Eq. 3.17)}$$

3.2. Equation of teff seed particle motion off- disc

A schematic of the off-spinner geometry is shown in *Fig*. 5 The spinner plate's height is assumed to remain constant and is located at a height *H*, above the ground. A particle is assumed to leave the spinner plate with the total velocity. The forces acting on a particle after it leaves the plate are assumed to include only gravitational forces, inertial forces and aerodynamic drag. The buoyancy force can be neglected since the density of air (about 1.2 kg/m^3) is much smaller than the density of the teff particle between 1275.21 kg/m^3 to 1361.35 kg/m^3 (Zewdu and Solomon, 2007). From Newton's Second Law, a particle's equations of motion are:

From fig.1 the discharge velocity is the resultant of the tangential velocity (v_t) and the radial velocity(v_r)

$$v_d = \sqrt{\left((\omega r)^2 + \left(\frac{dr}{dt}\right)^2\right)} \quad \text{(Eq. 3.18)}$$

Where $V_t = \omega r \ \ and \ V_r = \frac{dr}{dt}$ and form Fig.1 $V_r = \frac{dxv}{dt}\cos\beta$

And the discharge angle is

$$\theta = \tan^{-1}\left(\frac{Vt}{Vr}\right) \quad \text{(Eq. 3.19)}$$

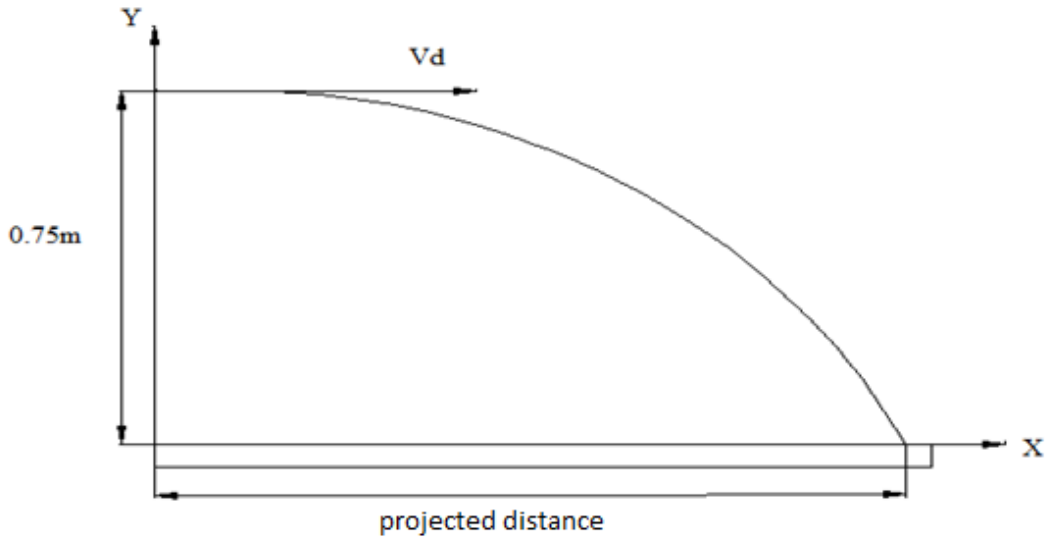

Figure 5: Trajectory of teff seed particles

$$m\ddot{x} = mg - \frac{1}{2}C_d\rho_a A_f V_r^2 \quad \text{(Eq. 3.20)}$$

Where x is the particle's position, C_d is the particle's drag coefficient, A_f is the particle's frontal-projected area,ρ_a is the surrounding air density, and g is the gravitational acceleration vector (assumed to act in the downward vertical direction).

The aerodynamic resistant coefficient of teff particle is given by

$$mg = \frac{1}{2}C_d\rho_a A_f V_r^2 \quad \text{(Eq.3.21)}$$

$$\frac{g}{V_r^2} = \frac{1}{2} C_d \frac{\rho_a}{m} A_f \quad \text{(Eq.3.22)}$$

$$K = \frac{1}{2} C_d \frac{\rho_a}{\rho_t V} A_f \quad \text{(Eq.3.23)}$$

Where

$K = \frac{g}{V_r^2}$ And $m = \rho_t V$

$$V = \frac{\pi d_e^3}{6} \quad \text{(Eq.3.24)}$$

$$A_f = \pi r^2 \quad \text{(Eq.3.25)}$$

$$d_e = \frac{r}{2} \quad \text{(Eq.3.26)}$$

Then substituting the above Eq.3.24, Eq.3.25 and Eq.3.26 into Eq.3.23

$$K = \frac{3}{4} C_D \frac{\rho_a}{\rho_t D_e} \quad \text{(Eq. 3.27)}$$

Where C_D particle is drag coefficient, ρ_a is air density, ρ_t is density of teff seed particles and D_e approximate diameters of *teff* seed particles. When moisture content is increased from 5.6% to 25.1% the drag coefficient of teff grain is decreased and the drag coefficient is linearly related to moisture content (Zewdu and Solomon, 2007).

$$C_D = -0.0074MC + 0.8627 \quad \text{(Eq. 3.28)}$$

Where MC is moisture content and C_d drag coefficient

Table 1: Physical and aerodynamic properties of *teff* seed

MC(%)	μ	D_e(m)	ρ_t(kg/m^3)
5.6	0.29	0.71×10^{-3}	1361.35
14.9	0.45	0.76×10^{-3}	1352.65
25.1	0.53	0.87×10^{-3}	1275.21

* Source: (Zewdu & Solomon, 2007)

Then equation (3.20) split into x and y components

$$\ddot{x} = -k\sqrt{(\dot{x}^2 + \dot{y}^2)}\dot{x} \quad \text{(Eq. 3.29)}$$

$$\ddot{y} = -k\sqrt{(\dot{x}^2 + \dot{y}^2)}\dot{y} - g \quad \text{(Eq. 3.30)}$$

Where x is the projected distance of the particle between the end of the vane and the location during the projectile motion, y is the vertical distance of the particle between the disc and the location during the projectile motion and g is the gravitational acceleration.

$$\frac{dx}{dt} = v_d \cos\theta \quad \text{(Eq. 3.25)}$$

$$\frac{dy}{dt} = v_d \sin\theta \quad \text{(Eq. 3.26)}$$

Where

θ is discharge angle, β is the pitch angle and v_o is the discharge velocity

4. Simulation of *teff* seed broadcaster

Equation 3.17, 3.23 and Eq. 3.24 describe the movement of teff seed particles from their first contact with disc until they land on the ground surface. Calculations of particle position are complex, so a program is developed in MATLAB SIMULINK blocks. The MATLAB SIMULINK enables us to tracking of the movement of *teff* seed particles along the vane. The MATLAB SIMULINK program also calculates the point at which the seeds leaves the disc and the location on the ground surface onto which it will land. During the motion of *teff* seed particle from the disc to ground surface, the speed and the direction of *teff* seed particle are the factors that have the greatest influence on the magnitude of the range of teff seed. Path of individual's teff seed particle and position of seed on the ground surface need to be known.

4.1. Simulation of *teff* seed on-disc

As input parameters, the disc radius (r) is 0.1 m, the disc rotational speed (wd), and the coefficient of friction between the teff seed and the surface on which it slides (μ) are entered in the MATLAB program. The result is a distribution pattern for a wide−angle teff seed spreader. On the basis of this distribution pattern, results can be evaluated and the initials conditions changed. Only one piece was simulated using different initial conditions. The results are presented below.

4.1.1. Motion of *teff* seed particles on spinning disc based on rotational speed of disc

The curve along which a teff seed particle travels varies with respect to the variation of the disc rotational speed, which was varied from 540 rpm to 1000 rpm. Variations of the disc rotational speed was affected the disc peripheral speed, so the speed with which seed leaves the disc increases as the disc rotational speed increases. To observe changes in the path of teff seed particle on the disc, a simulation of teff seed travel on the disc is performed at 540 rpm, 770 rpm and 1000 rpm (fig. 6). A comparison of the graphs (fig. 6) shows that at any rotational speed, the seed will cover a path ranging from 125° to 130°. The point at which the teff seed will depart from the disc will remain almost unchanged. The discharge velocity and discharge angle is calculated from Eq. 3.18 and Eq. 3.19 respectively. As shown in table 2 the discharge velocity

changed as the rotational speed of disc changed and a decrease of throwing time of *teff* seed particle.

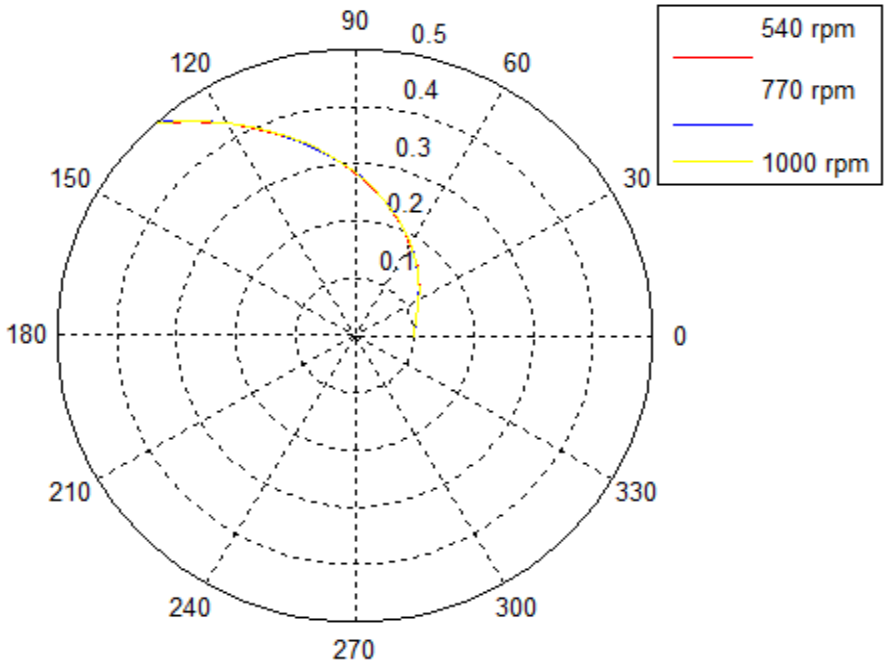

Figure 6: Trajectory of teff particle for various disc speeds,

r_0=0.1 m, $\alpha=0^0$ $\beta=0^0$& R=0.5m

	Disc rotational speed		
	540rpm	770rpm	1000rpm
Discharge velocity	35.04m/sec	50.02m/sec	64.43m/sec
Discharge angle	54.6	53.69	53.73

Table 2: Discharge angle and discharge velocity for various disc speeds

4.1.2. Motion of *teff* seed particles on spinning disc based on forward pitched angle

The motion of *teff* seed particles also depends on the pitch angle of vane which various in the forward direction. The initial position of the vane varies and the motion of teff seed on the disc is observed. The initial position of the vane moves from the disc's radial axis ($\beta=0^0$) upward to ($\beta=60^0$). Fig. 7 shows how the distance traveled on the disc by teff seed increase when the initial pitch angle is moved away. If the initial position of pitch vane angle is at $\beta=0^0$, then the disc must turn 135^0 for seed to reach the disc edge (fig.7). At $\beta=30^0$, the seed will need the disc to rotates over angle of 130^0 to reach the disc edge and also at $\beta=60^0$ the seed will need the disc to

rotates over angle of 125^0 to reach the disc edge. This results an slight increase of discharge velocity seed particles as the pitch angle of the vane increase as shown in table 3.

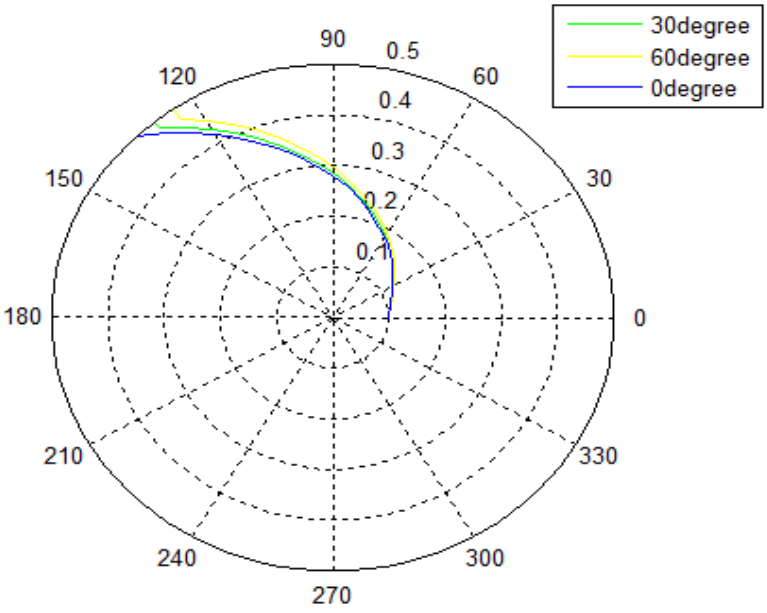

Figure 7: Trajectory of teff seed on disc for forward pitched angle,

r_0=0.1 m, N=770 rpm, $\alpha=0^0$ & R=0.5m

	Forward pitch angle		
	0	30	60
Discharge velocity	50.02m/sec	52.75m/sec	54.12m/sec
Discharge angle	53.69	52.75	57.86

Table 3: Discharge velocity and discharge angle for forward pitch angle

4.1.3. Motion of *teff* seed on spinning disc particles based on backward pitch angle

The motion of *teff* seed particles also depends on the pitch angle of vane which various in the backward direction. The initial position of the vane was varied and the motion of teff seed on the disc had been observed. The initial position of the vane was moved from the disc's radial axis ($\beta=0^0$) upward to ($\beta=-60^0$). The graphs in fig. 8 show how the distance traveled on the disc by teff seed increase when the initial pitch angle is moved away. If the initial position of pitch vane

angle is at $\beta=0^0$, then the disc must turn 135^0 for seed to reach the disc edge (fig.8). At $\beta=-30^0$, the seed will need the disc rotates over angle of 140^0 to reach the disc edge and also at $\beta=-60^0$ the seed will need the disc to rotates over angle of 170^0 to reach the disc edge. These results slight decreases of discharge velocity of *teff* seed particles as the pitch angle of the vane increase as backward direction as shown in table 4.

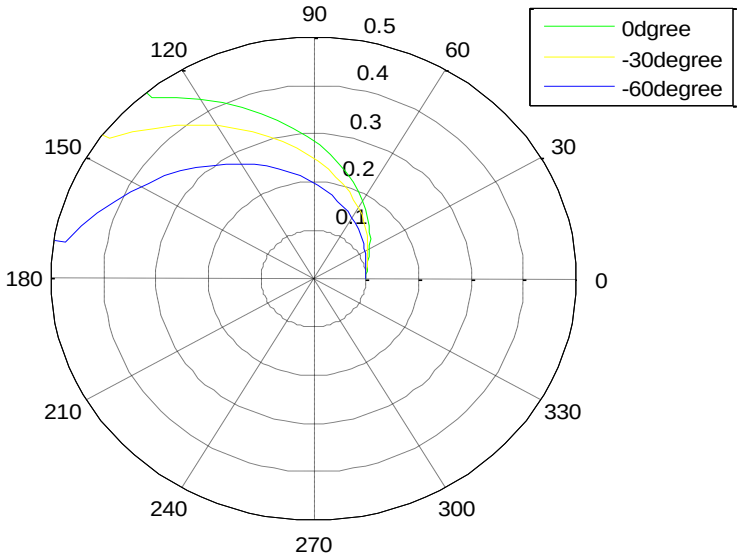

Figure 8: Trajectory of teff seed on disc for various backward pitched angles, r_0=0.1 m, N=770 rpm, $\alpha=0^0$ & R=0.5m

	Backward pitched angle		
	0	-30	-60
Discharge velocity	50.02m/sec	46.57m/sec	43.308
Discharge angle	53.69	53.57	55.19

Table 4: Discharge velocity and discharge angle for backward pitch angle

4.1.4. Motion of *teff* seed particles on spinning disc with varying coefficient of friction

Varying the moisture content of teff seed particle which has different coefficients of friction between the teff seed particle and the surface on which the teff slides. The influence of the

coefficient of friction on the movement of teff seed particle on the disc was observed. Three values of the coefficient of friction were used (fig. 9), from μ= 0.29 to μ = 0.53 (Zewdu, 2008). Simulation showed that the path length of travel increases with an increase in the coefficient of friction. At μ= 0.29, the teff seed rotates around the axis of disc rotation for about 115°, at μ= 0.45 the angle is 130°, and at μ= 0.53 it is 135°. The coefficient of friction thus exerts an influence on the distance a teff seed particle travels on the disc and consequentially on the point from which it leaves the disc. An increase of coefficient of friction as shows in table 5 will be slightly decreasing the discharge velocity.

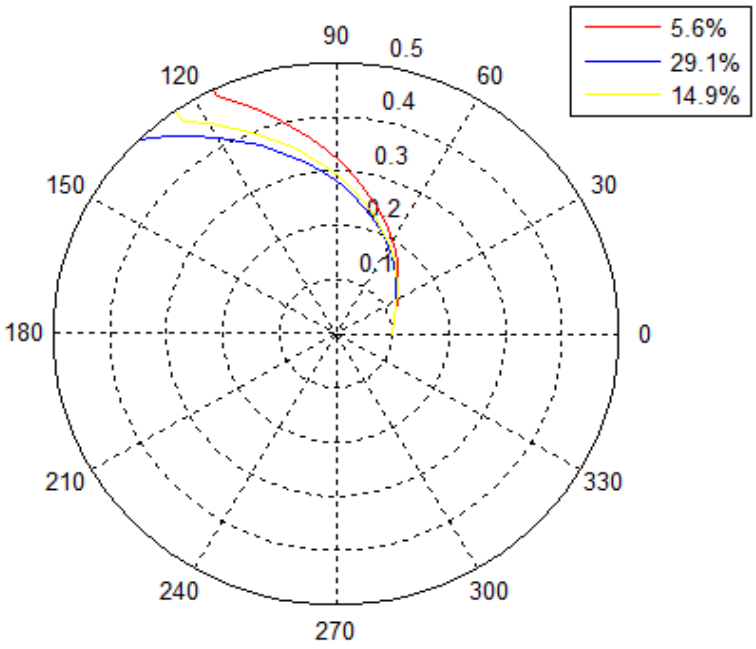

Figure 9: Trajectory of teff seed on disc for various moisture contents,

r_0=0.1 m, N=770 rpm, α=0^0 & R=0.5m

	Moisture content		
	5.6%	14.9%	29.1%
Discharge velocity	53.716m/sec	50.8m/sec	49.57m/sec
Discharge angle	48.6	52.48	54.38

Table 5: Discharge velocity and discharge angle for various moisture contents

4.1.5. Motion of *teff* seed particles on spinning disc based on cone angle of disc

The motion teff seed particle is also depends on the cone angle of the disc which is varies. The cone angle of disc varies from $\alpha=0^0$ to upward $\alpha=15^0$ and the motion of teff seed is observed. The Fig.10 shows the particle trajectory on the disc, increased the point where teff seed leave the disc when the cone angle was increased. If the cone angle $\alpha=0^0$ which is flat, then the disc must turn 135^0 for seed to reach the disc edge (fig.10). At $\alpha=5^0$, the seed will need the disc to rotates over angle of 145^0 to reach the disc edge and at $\alpha=15^0$ the seed will need the disc to rotates over angle of 150^0 to reach the disc edge.

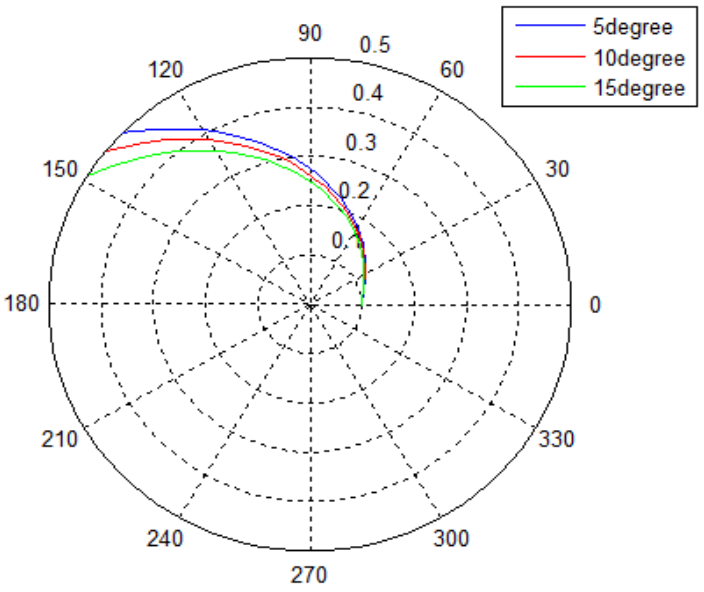

Figure 10: Trajectory of teff seed particle on disc various cone angles,

r_0=0.1 m, N=770 rpm, $\beta=0^0$ & R=0.5m

	Cone angle		
	5	10	15
Discharge velocity	49.41m/sec	48.637m/sec	47.917m/sec
Discharge angle	54.63^0	55.87^0	57.27^0

Table 6: Discharge velocity and discharge angle for various cone angle

4.2. Simulation *teff* seed trajectory off-disc

Once a teff seed has left the disc, its point of release from the disc and the location on the ground are known. The principle of projectile motion is used for calculating the path (Eq. 3.29) and (Eq.3. 30). The range of the teff seed depends primarily on its speed and the vertical distance between the place of release from the disc and the ground surface (*h* in fig. 5).

Simulation of teff seed spreading is done by MATLAB-SIMULINK program using findings from previous analyses of teff seed motion on the disc as an initial condition for teff seed off-disc trajectory.

4.2.1. Motion of *teff* seed particles off disc based on rotational speed of disc

The off disc motion of *teff* seed particle depends on the rotational speed of disc as shown in fig. 11. The increase of rotational speed of disc will also increase the horizontal distance to be projected. When the rotational speed is 540 rpm, the *teff* seed will be projected to nearly 4.25 m and as the rotational speed increased to 770 rpm, the teff seed will projected to nearly to 4.75 m. At 1000 rpm, the teff seed particle projected to nearly to 5 m projected distance.

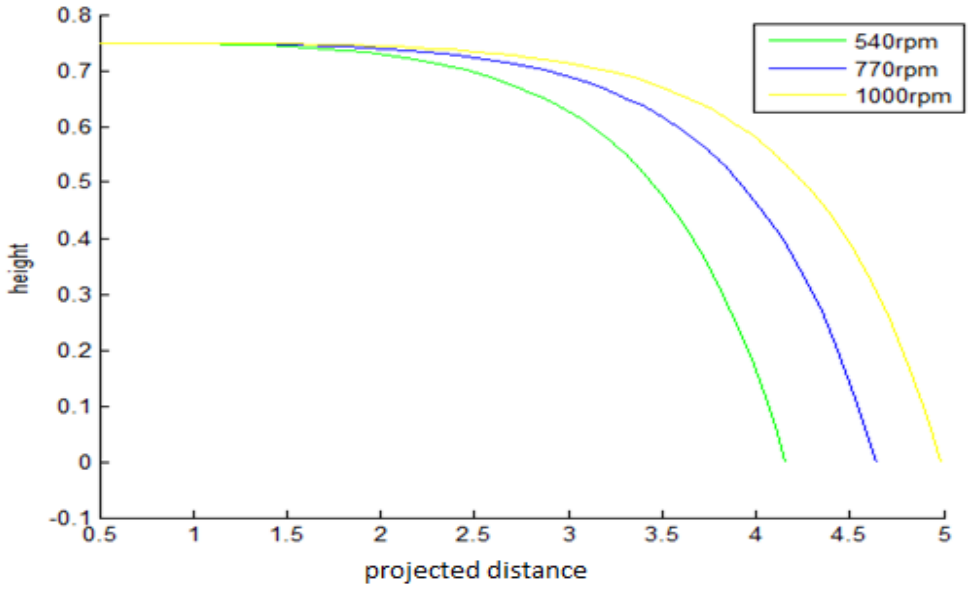

Figure 11: Projected distance versus Height with varying disc rotational speed

$\beta=0^0$, r=0.1 m, R=0.5 m & $\alpha=0^0$

4.2.2. Motion of *teff* seed particles off disc based on forward pitch and backward pitch angle

As the increase of forward pitch angle of vane will also slightly increase the projected distance of teff seed particle. When the forward pitch angle is 30^0, the projected distance of teff seed is nearly 4.75 m as shown in Fig. 12 and at 60^0, the distance to be projected is nearly 4.8 m. But in the case of backward pitch angle, the increase of pitch angle of vane will decrease the projected distance of teff seed particle as shown in Fig. 13. When the pitch angle is -30^0, the teff seed particle will project nearly 5.6 m and at -60^0, the teff seed will projected to nearly 4.5 m. When comparing the two pitch angle in case of forward pitch angle the teff seed will higher projected distance as that of backward pitch angle.

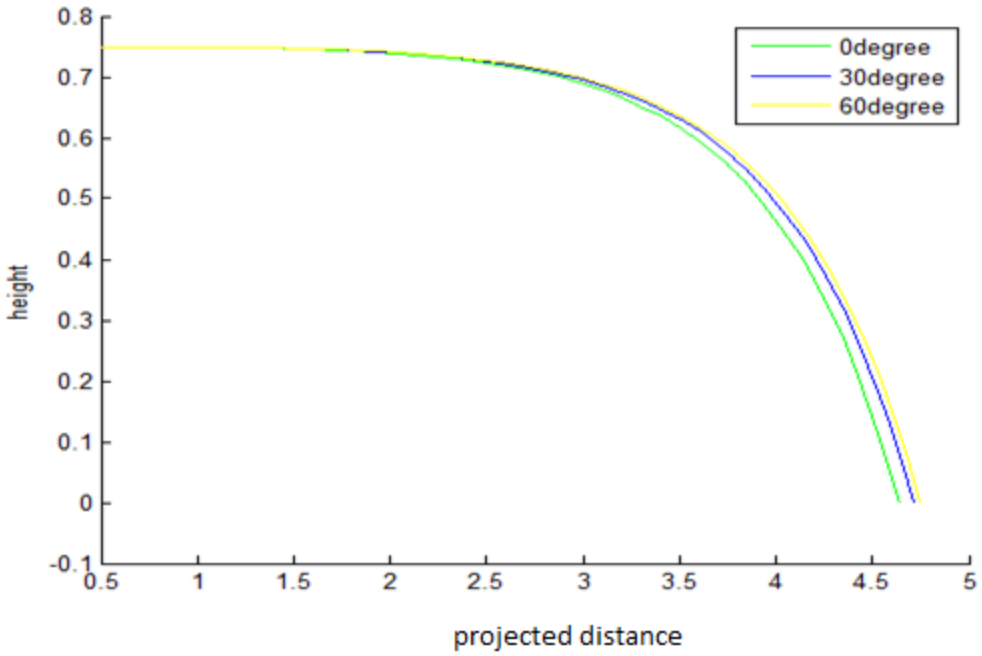

Figure 12: Height versus projected distance in forward pitch vane angle, N= 770 rpm, r=0.1 m, R=0.5 m & $\alpha=0^0$

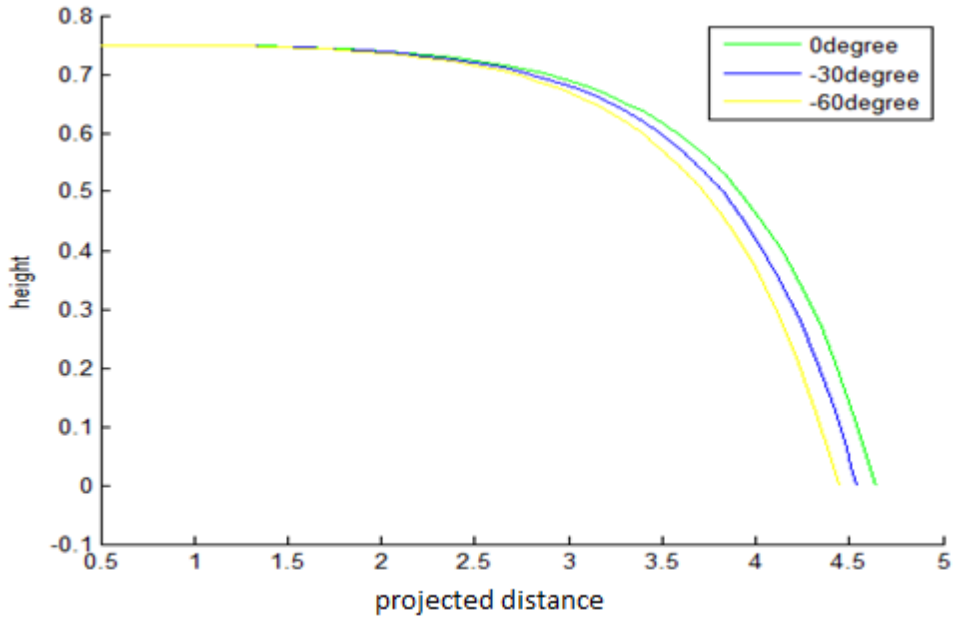

Figure 13: Height versus projected distance in backward pitched vane angle, N=770rpm, r=0.1m, R0.5 m & $\alpha=0^0$

4.2.3. Motion of *teff* seed particles off disc based on moisture contents

Projected distance and particle motion of t*eff* seed with different moisture content is as shown in Fig. 14. As moisture content is increase the projected distance will also increase even if the discharge velocity is decrease this is due to the increase of air drag coefficient and the mass of thousand teff seed is increase (Zewdu & Solomon, 2010). When the moisture content of teff seed is 5.6%, the projected distance is approximately 4.6m and at 14.95% the teff seed particle will projected approximately 4.75 m and when the moisture content is 25.1%, the projected distance of teff seed is nearly 5 m.

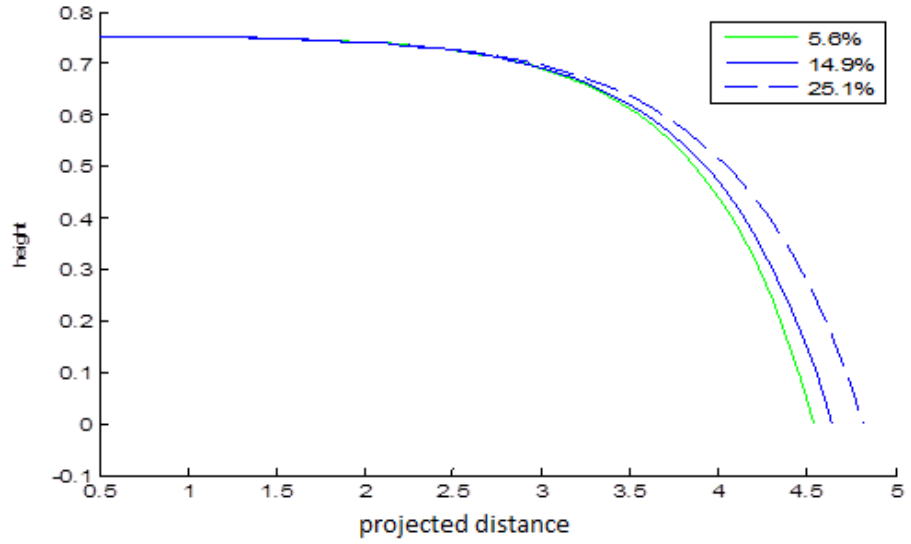

Figure 14: height versus projected distance at varying moistures content,

N=770 rpm, r0.1 m, R=0.5 m & β=0^0

4.2.4. Motion of *teff* seed particles off disc based on cone angle of disc

The Fig. 15 shows the trajectory of teff seed particle and the projected distance. It is clearly seen the projected distance of teff seed particle is increased as the increase of the cone angle of disc. When the cone angle is 5^0, the teff seed will be projected nearly to 5 m and when the cone angle is 10^0, the teff seed particle is projected to 5.2 m and at 15^0, the projected distance is nearly 5.3 m

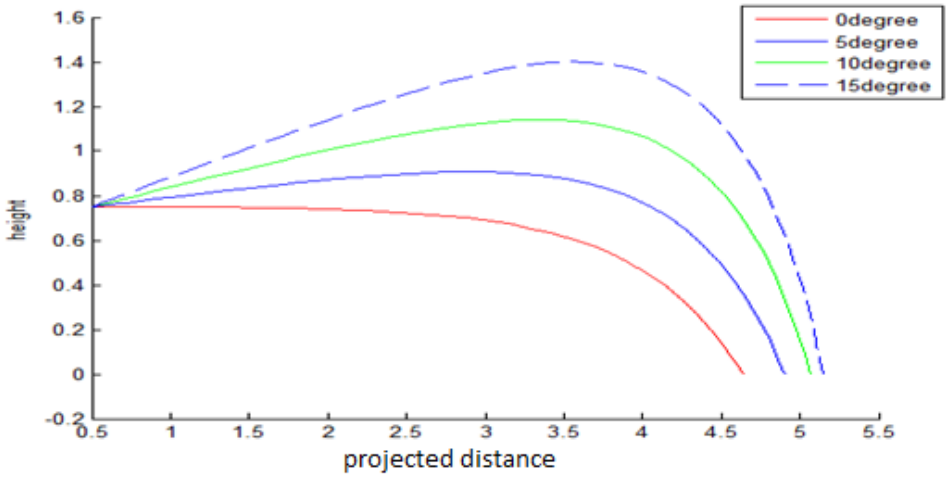

Figure 15: Height versus projected distance at varying cone angles,

N=770 rpm, r=0.1 m, R=0.5 m & β=0^0

5. Machine parts design

5.1. Hopper design

The hopper is designed to be feed in a vertical position only. The material used for the construction is mild steel sheet metal with thickness 3 mm, which is readily available in the market and relatively affordable. The hopper has the shape of a frustum of a truncated cone at the bottom, with top and bottom having circular forms. This type of hopper is a gravity discharge one, and the recommended angle of repose for gravity discharge of teff is 51.6^0 at a moisture content of 25.1% (Zewdu and Solomon, 2007) and they also found the bulk density of *teff* seed 768kg/m^3.

So in this case the angle of repose 60^0 because to ensure the free flow of teff seed and we take design assumption that is the hopper hold 90 kg of teff seed at a time to cover a 3 hector coverage if the application rate is 30 kg/ha, the top diameter of the hopper 1000 mm, the bottom diameter 250 mm. From this assumption it is possible to find the volume of the hopper and other parameters.

$$V = \frac{m}{\rho} = \frac{90}{768} \qquad \text{(Eq. 5.1)}$$

Then the total volume of the hopper

$V = 0.1172\ m^3$

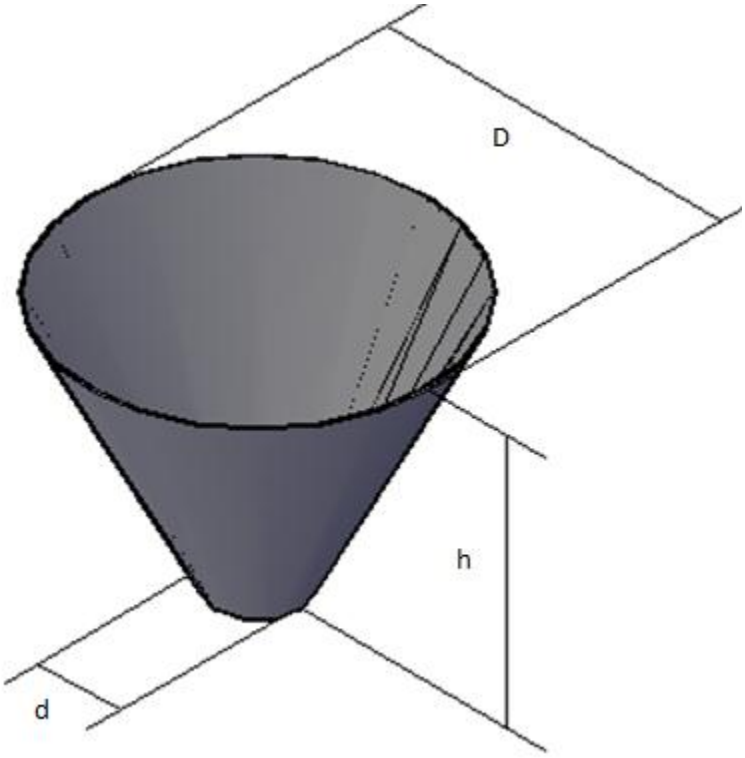

Figure 16: Designed Hopper

$$V = \frac{\pi(D^2 - d^2)h}{12} \qquad \text{(Eq.5.2)}$$

$$0.1172 = \frac{\pi(1^2 - 0.25^2)h}{12}$$

Then, the height of the hopper

$$h = 500\ mm$$

$$h = l\cos\emptyset$$

$$l = \frac{h}{\cos\emptyset} = \frac{500\ mm}{\cos 60} = 1000\ mm$$

5.2. *Teff* rate of discharge from hopper

According to Johanson (1965) he found the fundamental equation of the mass flow rate of coarse particles (particles greater than500micros) is given by

$$\dot{m} = \rho A \sqrt{\frac{Bg}{2(1+m)\tan\theta}} \qquad \text{(Eq.5.3)}$$

Where

$\dot{m}$ Mass flow

ρ bulk density

θ semiincluded angle of hopper (repose angle)

Table 7: Parameters in Johanson's equation

Parameters	Conical hopper	Symmetrical slot hopper
B	D	W
A	$\pi D^2/4$	WL
M	1	0

* **Source: Johanson (1965)**

The working speed of the tractor is 8 km/h (2.22 m/sec), in one second the flow rate will

0.066kg/sec

To find the outlet of the hopper from Eq.5.3

In this case the hopper is conical shape from table 7 the value of the parameter

$B = D$ And $A = \frac{\pi D^2}{4}$

Then, the above value substituted to Eq.5.3

$$0.066 = 768 \times \frac{\pi D^2}{4} \sqrt{\frac{D \times g}{2(1+1)\tan 60}}$$

$D_o = 24.3\ mm$

5.3. Spinning disc and vanes

Teff seed which pass through hopper and reached the disc with 1 m diameter and made of mild steel flat sheet metal with 5 mm thickens and also four straight vanes are attached on disc by 8 M6 bolts and the length of each vane is 400 mm, 5 mm thickness, 40 mm width, 40 mm height and made of mild steel flat sheet metal

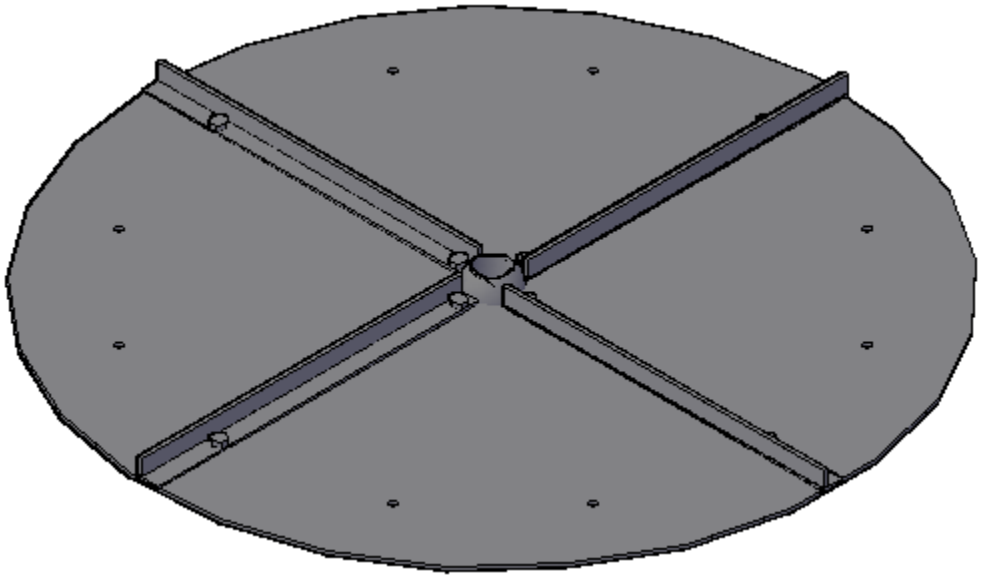

Figure 17: Assembly of disc and vane

5.4. Design of bevel gear

Bevel gears transmit power between two intersecting shafts at any angle or between non-intersecting shafts. A bevel gear pair has to be designed to transmit 253 hp or188 kW power at 1000 rpm. The shaft angle is 90^{o}. Speed ratio desired is about 1. The prime mover is tractor output and the driven side is connected to a spinning disc. Different assumptions are taken in to account to design a bevel gear as fellow.

1. The gears are to be mounted on anti-friction bearings in a gear box and are subjected to light shock due to sudden loading of the teff seed particle on disc.
2. The gearbox has to last for 20 years for which hardened gears are selected.
3. The gears are of continuous duty and one gear straddle mounted on antifriction ball bearings and other is overhung.
4. The pinion material is made of C45 steel of hardness 380 Bhn and tensile strength σ_{ut}= 1240 MPa. The gear is made of ductile iron grade 120/90/02 of hardness 331 Bhn and tensile strength σ_{ut}= 974 MPa.
5. A factor of safety of 1.5 and 1.2 on bending and contact fatigue strengths of the materials is assumed respectively.

$N = 1000\ rpm$	$\sigma_{utG} = 927MPa$
$i = 1$	$fs_b = 1.5$
$P = 188\ kw\ or\ 253\ hp\ \ pto\ output$	$fs_f = 1.2$
$\sigma_{utp} = 1240MPa$	$\text{Hardness}_{pinion} = 380Bhn$

Table 8: Parameters used in the design of bevel gear

First to determine the allowable stresses of the pinion and gear material

For pinion material

$\sigma_{utp} = 1240MPa$

$\text{Hardness}_{pinion} = 380\ Bhn$

Then from table 9

$\sigma'_{sf} = 2.8(Bhn) - 69\ MPa$ (Eq. 5.4)

Substituting the above value into equation 5.4

$\sigma'_{sf} = 2.8(380) - 69\ MPa$

$\sigma'_{sf} = 995\ Mpa$

Source: (Richard et al, 2008)

Material	$\sigma'_{sf}(MPa)$
Steel	2.8(Bhn)-69MPa
Nodular Iron	0.95[2.8(Bhn)-69]MPa
Cast Iron, grade 20	379
Cast Iron, grade 30	482
Cast Iron, grade 40	551
Tin Bronze, AGMA 2C(11%Sn)	207
Aluminum Bronze (ASTM B 148-52) (Alloy 9C-H.T)	448

Table 9: Surface fatigue strengthσ'_{sf} (MPa) for metallic bevel gears (10^7 cycle life, 99% reliability and temperature <120 ^{o}C)

Corrected bending fatigue strength of the pinion material:

$\sigma_e = \sigma'_e K_L K_V K_S K_r K_T K_f K_m$ (Eq. 5.5)

$\sigma'_e = 0.5\ \sigma_{utp} = 0.5 * 1240\ MPa = 620\ MPa$

$K_L = 1.0$ For bending

$K_V = 1.0$ for bending for $m \leq 5\ module$

$K_S = 0.645$ for $\sigma_{utp} = 1240 Mpa$ from figure 17

$K_r = 0.897$ for 90% reliability from table 10

$K_T = 1.0$ with temperature less than 120 ^{o}C, $K_f = 1.0$

$K_m = 1.33$ for $\sigma_{utp} = 1240\ Mpa$ from figure 18

Then the above all value substitute into equation 5.5

$\sigma_e = 620 * 1 * 1 * 0.645 * 1 * 1 * 0.897 * 1.33Mpa$

$\sigma_e = 477MPa$

Source: (Richard et al, 2008)

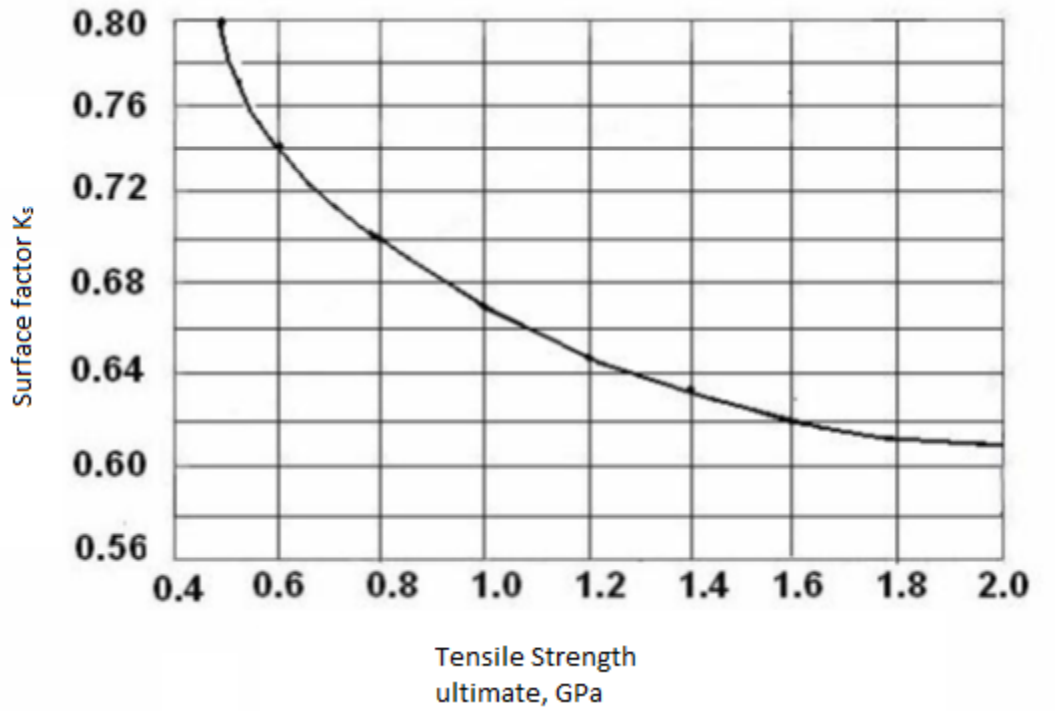

Figure 18: Surface factor, k_s

Table 10: Reliability factor k_r

Reliability factor R	0.5	0.9	0.95	0.99	0.999	0.9999
Factor K_r	1.000	0.897	0.868	0.814	0.753	0.702

*Source: (Richard et al, 2008)

Source: (Richard et al, 2008)

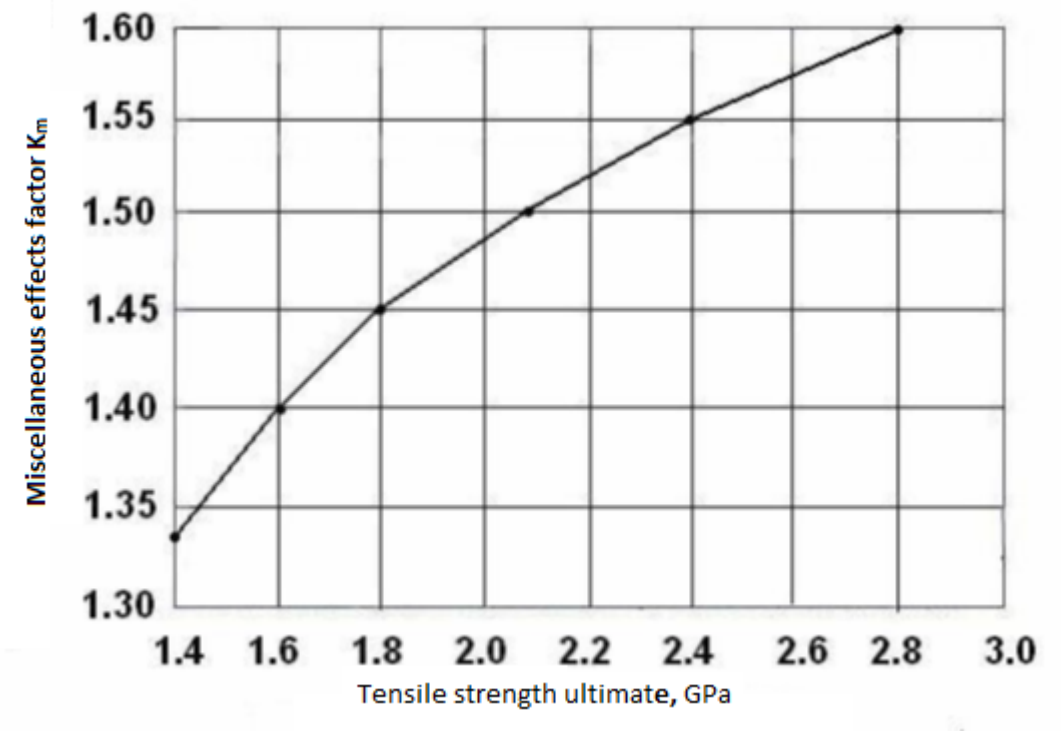

Figure 19: Miscellaneous effect factor, K_m

Corrected fatigue strength of the gear material:

$\sigma_e = \sigma_e' K_L K_V K_S K_r K_T K_f K_m$ (Eq.5.6)

$\sigma_e' = 0.5\sigma_{utp} = 0.5 * 974MPa = 340.9MPa$

$K_L = 1.0$ for bending

$K_V = 1.0$ for bending for $m \leq 5$ *module*

$K_S = 0.645$ for $\sigma_{utp} = 1240$ Mpa from figure 17

$K_r = 0.897$ for 90% reliability from table 10

$K_T = 1.0$ with temperature less than 120^{o}C, $K_f = 1.0$

$K_m = 1.33$ for $\sigma_{utp} = 1240$ Mpa from figure 18

Then the above all value substitute into equation 5.5

$\sigma_e = 340.9 * 1 * 1 * 0.645 * 1 * 1 * 0.897 * 1.33$ Mpa

$\sigma_e = 292.44$ MPa

Surface fatigue strength of pinion

$\sigma_{sf} = \sigma'_{sf} K_L K_H K_R K_T$ (Eq.5.7)

For table 9

$\sigma'_{sf} = 2.8(Bhn) - 69MPa$

$\sigma'_{sf} = 2.8(380) - 69MPa$

$\sigma'_{sf} = 995MPa$

$K_L = 0.9$ for 10^8 cycles from Fig.19

Source: (Richard et al, 2008)

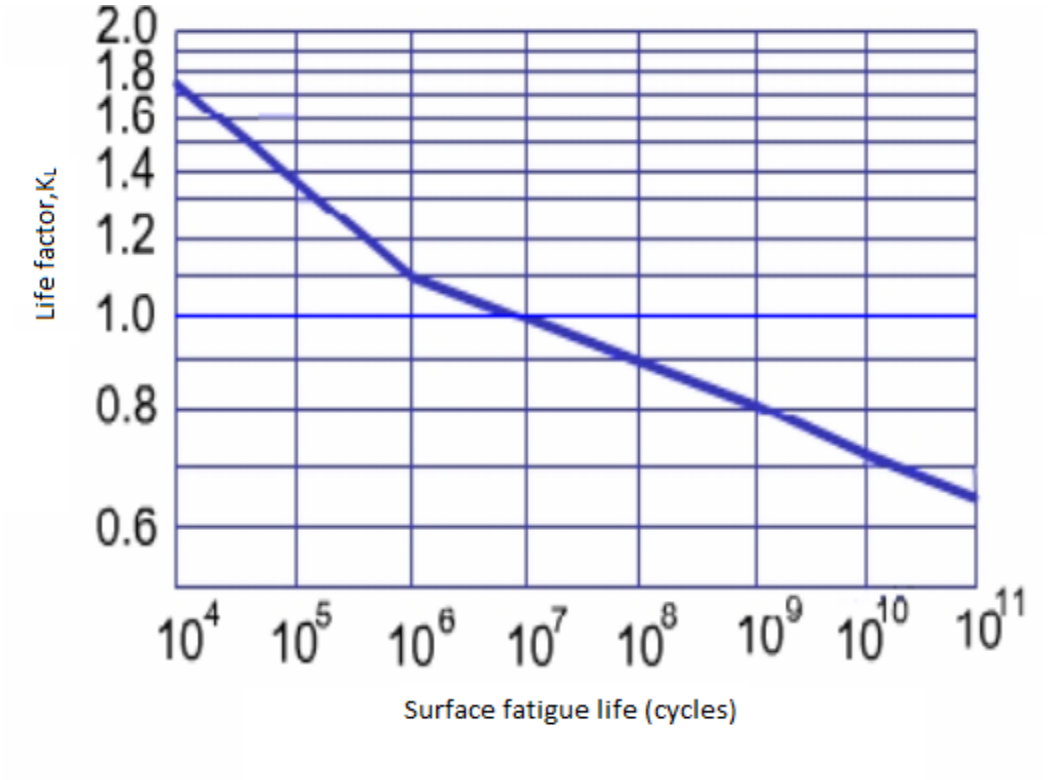

Figure 20: Life factor, K_L

$K_H = 1 \text{for} K = {}^{380}/_{331} = 1.14$ from figure 20 K is Brinell hardness ratio of pinion and gear and $K_H = 1$ for values of K below 1.2

Source: (Richard et al, 2008)

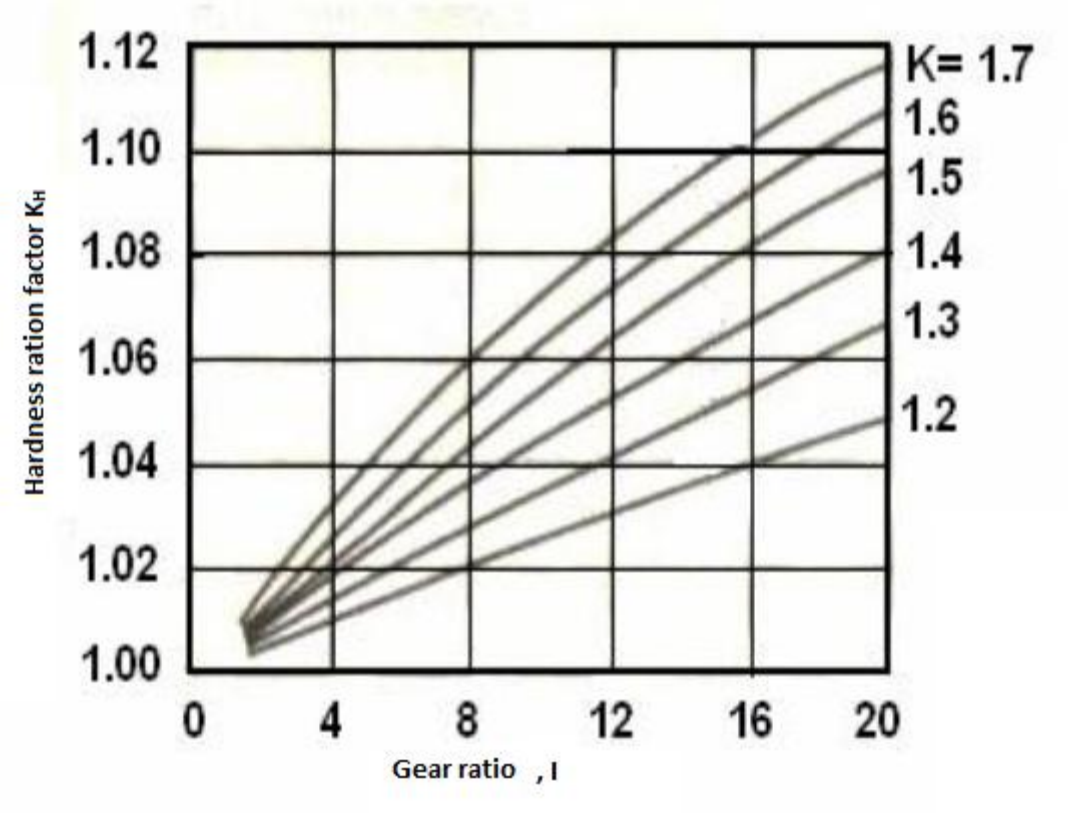

Figure 21: Hardness ration factor, K_H

Table 11: Reliability factor K_R

Reliability(%)	50	99	99.9
K_R	1.25	1.0	0.80

Source: (Richard et al, 2008)

$K_R = 1.0$ for 99% reliability from table 11

$K_T = 1$ for temperature less than $120^0 c$

Then the above all values substitute into equation (Eq.5.7)

For pinion material

$\sigma_{sf} = 995 * 0.9 * 1 * 1 * 1$

$\sigma_{sf} = 895.5MPa$

For gear

$\sigma'_{sf} = 0.95(2.8(Bhn) - 69)MPa$ From table 9 (Eq.5.8)

$\sigma'_{sf} = 0.95(2.8(331) - 69)MPa$

$\sigma'_{sf} = 815Mpa$

$K_L = 0.9$ for $8.15*10^8$ cycles from Fig.21

$K_H = 1$ for$K = {}^{380}/_{331} = 1.14$ from figure 20 K is Brinell hardness ratio of pinion and gear and $K_H = 1$ for values of K below 1.2

$K_R = 1.0$ for 99% reliability from table 10

$K_T = 1$ for temperature less than 120^0c

The substitute all the above values into equation 5.7

$\sigma_{sf} = 815 * 0.9 * 1 * 1 * 1$

$\sigma_{sf} = 733.5\ MPa$

Permissible stresses in bending fatigue

Pinion material: $[\sigma_{Pb}] = \frac{\sigma_e}{fsp} = \frac{477}{1.5}$

$\sigma_{Pb} = 318MPa$

Gear material:$[\sigma_{Gb}] = \frac{\sigma_e}{fsp} = \frac{292.44}{1.5}$

$\sigma_{Gb} = 194.96\ MPa$

Permissible stresses in contact fatigue

Pinion material: $[\sigma_{Pf}] = \frac{\sigma_{sf}}{fsp} = \frac{895.5}{1.2}$

$\sigma_{Pf} = 746.25\ MPa$

Gear material: $[\sigma_{Pb}] = \frac{\sigma_{sf}}{fsp} = \frac{815}{1.2}$

$\sigma_{Gf} = 679.16\ MPa$

$Z_1 = 20$ assumed for 20^0pressure angle gears.

$Z_2 = iZ_1 = 1 * 20$

$Z_2 = 20$ to have hunting tooth action, the value of $Z_2$is taken to be 21

Hence $i = \frac{Z_2}{Z_1} = \frac{21}{20} = 1.016$

$N_2 = \frac{N_1}{i} = \frac{1000\ rpm}{1.016}$

$N_2 = 943.99 rpm$

$\tan\gamma_1 = \frac{Z_1}{Z_2} = \frac{20}{21}$, hence $\gamma_1 = 43.6^0$

$\gamma_2 = £ - \gamma_1 = 90° - 43.6°$

$\gamma_2 = 46.4°$

$\omega_1 = \frac{2\pi N_1}{60} = \frac{2*\pi*1000}{60}$

$\omega_1 = 104.71\ {}^{rad}/_{sec}$

$Torque =\ T_1 = \frac{power}{\omega_1} = \frac{11.19kw}{104.71}$

$T_1 = 107.49\ Nm$

Bending stress in pinion

$$\sigma_{b1} = \frac{F_t}{bmJ} K_V K_o K_m \quad \text{(Eq.5.9)}$$

Assuming b=8m

Where,

$$F_t = \frac{2\pi}{d_1} \quad \text{(Eq.5.10)}$$

$$d_1 = mZ_1 \quad \text{(Eq.5.11)}$$

Then, substituting equation 5.10and 5.11 into 5.9

$$\sigma_{b1} = \frac{2T_1}{8m^3 Z_1 J} K_V K_o K_m \quad \text{(Eq.5.12)}$$

$$Z_{V1} = \frac{Z_1}{\cos \gamma_1} = \frac{20}{\cos 43.6°}$$

$$Z_{V1} = 27.6$$

$$Z_{V2} = \frac{Z_2}{\cos \gamma_2} = \frac{21}{\cos 46.4°}$$

$$Z_{V2} = 30.45$$

$J = 0.27$ for $Z_{V1} = 27.6$ mating against $Z_{V2} = 30.45$ from figure 21

Source: (Richard et al, 2008)

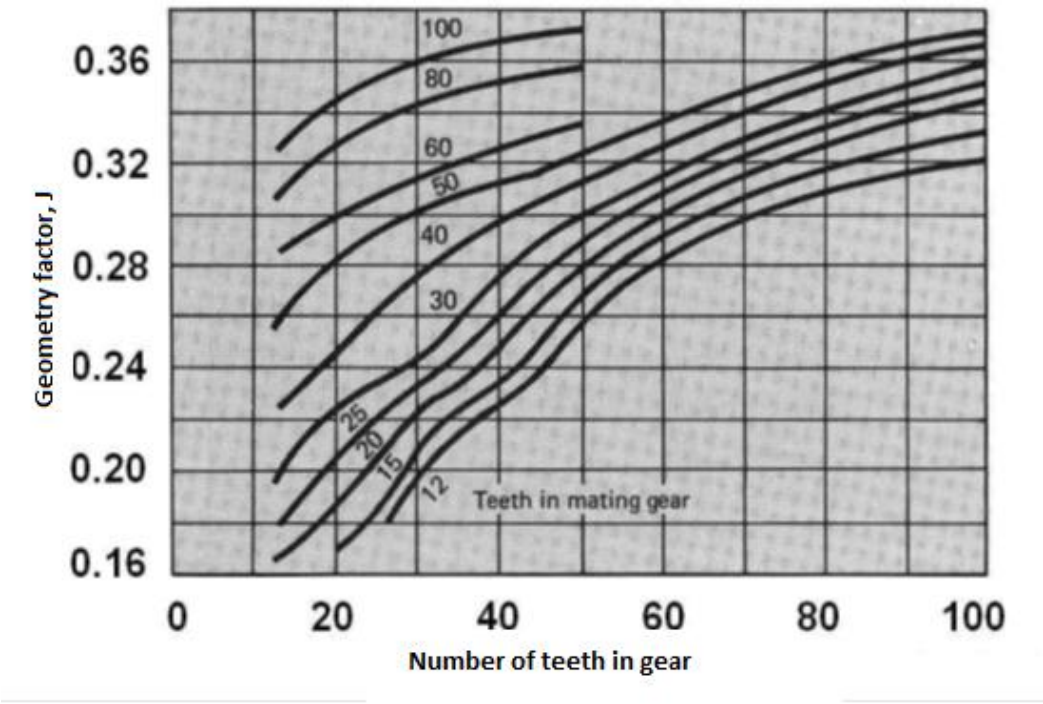

Figure 22: Number of teeth in gear for which geometry factor J is desired, pressure angle

$K_V = 1.25$ assumed expecting the V to be 8 m/s from Fig.24

Source: (Richard et al, 2008)

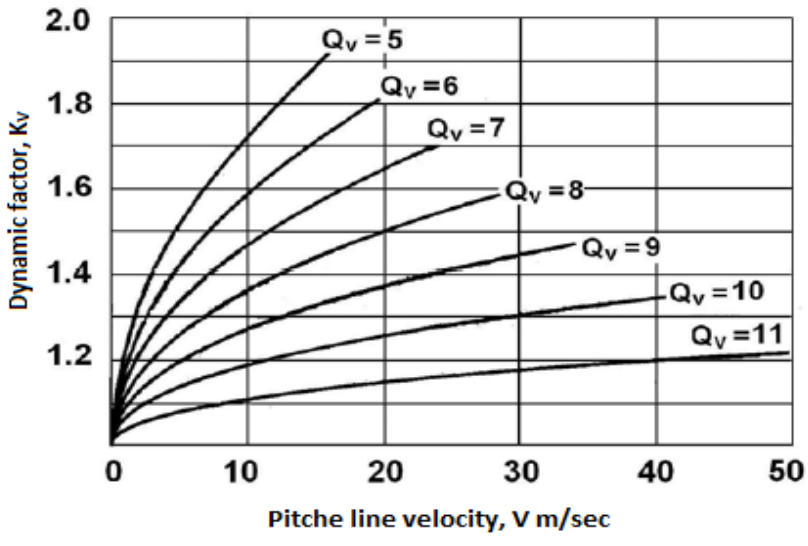

Figure 23: Dynamic load factor,K_V

$K_o = 1.75$ Medium shock and driven is medium shock from table 12

Table 12: Overload factor K_o

	Driven machinery		
Source of power	Uniform	Moderate shock	Heavy shock
Uniform	1.00	1.25	1.75
Light shock	1.25	1.50	2.00
Medium shock	1.50	1.75	2.25

*Source: (Richard et al, 2008)

$K_m = 1.4$ one gear straddle mounted and the other overhung from fig.23

Source: (Richard et al, 2008)

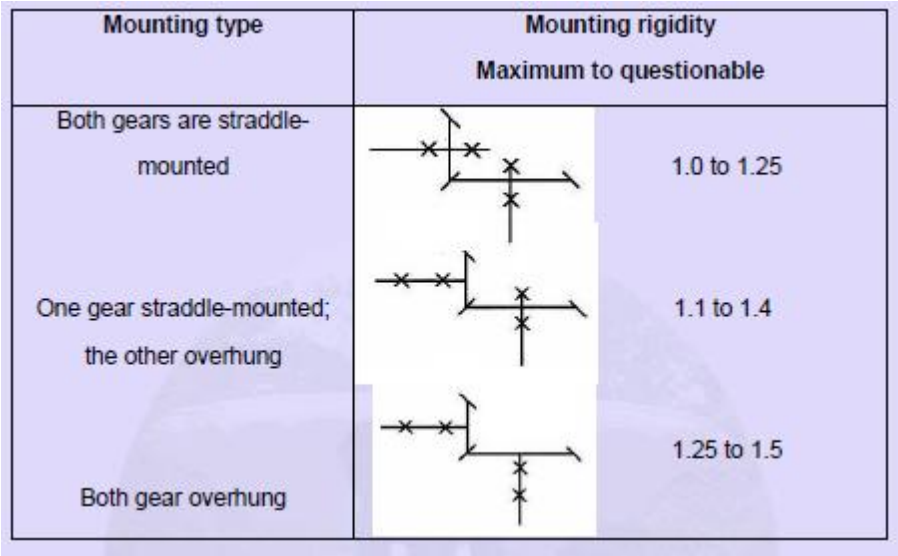

Figure 24: Bevel gears-mounting factor K_m

Substitute all above value into equation (Eq.4.9)

$$\sigma_{bp} = \frac{2T_1}{8m^3 Z_1 J} K_V K_o K_m = \frac{2 \times 107.49 \times 1000}{8m^3 \times 20 \times 0.27} \times 1.25 \times 1.75 \times 1.4$$

$$\sigma_{bp} = \frac{61.9}{m^3} MPa \quad \text{(Eq. 5.13)}$$

$$\sigma_{b1} \leq [\sigma_{Pb}] \quad \text{(Eq.5.14)}$$

$$\frac{9929.66}{m^3} \leq 318 \quad \text{(Eq.4.12)}$$

$$m = 3.63\ mm$$

Similarly for gear

$J = 0.27$ for $Z_{V1} = 27.76$ mating against $Z_{V2} = 30.45$ from figure 21

K_o , K_m *and* K_v are similar to the pinion material

$$\sigma_{bG} = \frac{2T_1}{8m^3 Z_1 J} K_V K_o K_m = \frac{2 \times 107.49}{8m^3 * 21 * 0.27} \times 1.25 \times 1.75 \times 1.4$$

$$\sigma_{bG} = \frac{11.87}{m^3} MPa \quad \text{(Eq.5.15)}$$

$$\sigma_{bG} \leq [\sigma_{PG}] = 194.96\ MPa \quad \text{(Eq.5.16)}$$

$$\frac{11870}{m^3} \leq 194.96\ Mpa \quad \text{(Eq.5.17)}$$

$$m = 4.206\ mm$$

Then take the standard module 5mm

$$m = 5\ mm$$

$$b = 8 \times m = 8 \times 5\ mm = 40\ mm$$

$$d_1 = mZ_1 = 5 \times 20 = 100\ mm$$

$$L = \frac{d_1}{\sin \gamma_1} = \frac{100\ mm}{\sin 43.6} = 145\ mm$$

$b < \frac{L}{3} = \frac{145}{3} = 48\ mm$ It satisfies the requirements

$$F_t = \frac{2T_1}{d_1} = \frac{2 * 107.49}{0.1} = 2149.8\ N$$

$$V_1 = \omega_1 r_1 = 104.71 \times 0.05$$

$$V_1 = 5.23\ {}^{m}/_{sec}$$

Bevel gear contact stress

$$\sigma_H = C_p \sqrt{\frac{C_p}{bdI} K_V K_o K_m} \qquad \text{(Eq.5.18)}$$

$C_P = 166$ From table 13

Table 13: Elastic Coefficient Cp for bevel gears, in MPa$^{0.5}$

Pinion material (μ=0.3 in all cases)	Gear material			
	Steel	Cast Iron	Al Bronze	Tin Bronze
Steel, E=207Gpa	191	166	162	158
Cast Iron, E=131Gpa	166	149	149	145
Al Bronze, E=121Gpa	162	149	145	141
Tin Bronze, E=110Gpa	158	145	141	137

*Source: (Richard. et al, 2008)

$I = 0.075$ from figure 26

Source: (Richard et al, 2008)

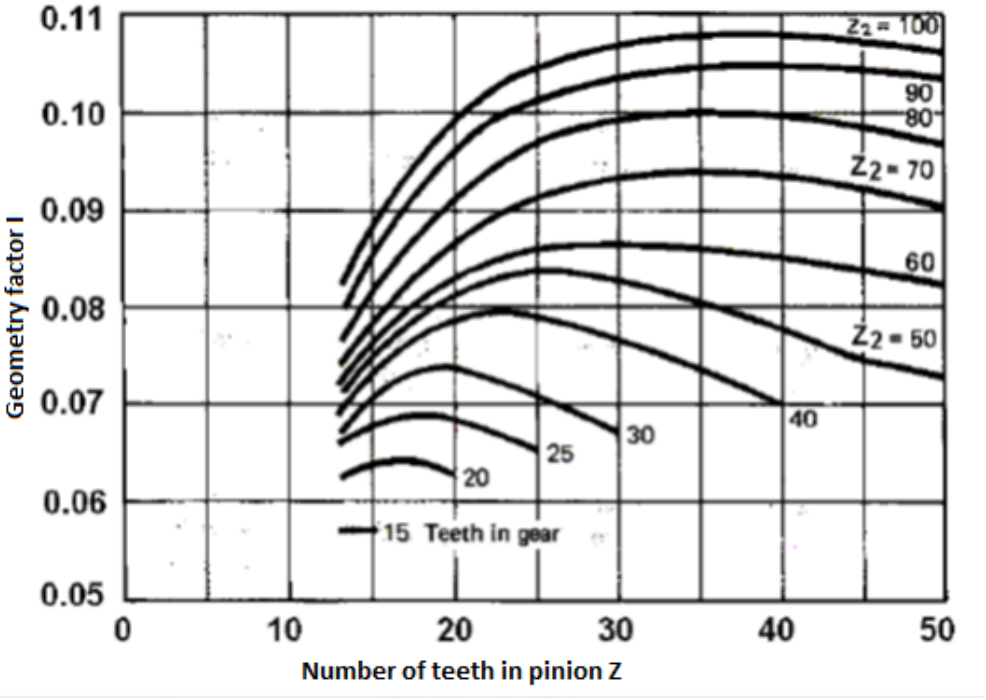

Figure 25: Geometry factor I for straight bevel gear pressure angle 20^0 and shaft angle 90^0

$K_V = 0.75$For V = 5.23 m/s from Fig. 22, for quality 10 gears

Other factors are the same with that of bending stresses analysis

$K_0 = 1.75$

$K_m = 1.4$

Substitute all the above into equation 4.16

$$\sigma_H = 166\sqrt{\frac{2149.8}{40 \times 100 \times 0.075} \times 0.75 \times 1.75 \times 1.4}$$

$\sigma_H = 580.59\ Mpa$

$[\sigma_{Pf}] = 746.25\ Mpa$ And $[\sigma_{Gb}] = 679.16\ MPa$

$\sigma_H < [\sigma_{Gb}]$ *or* $[\sigma_{Pb}]$. Therefore the bevel gear design is safe

5.5. Shaft design and analysis

A shaft is the component of a mechanical device that transmits rotational motion and power. It is integral to any mechanical system in which power is transmitted from a prime mover, such as an electric motor or an engine, to other rotating parts of the system. There are many examples of mechanical systems incorporating rotating elements that transmit power: gear-type speed reducers, belt or chain drives, conveyors, pumps, fans, agitators, household appliances, lawn maintenance equipment, parts of a car, power tools.

Visualize the forces, torques, and bending moments that are created in the shaft during operation. In the process of transmitting power at a given rotational speed, the shaft is inherently subjected to a torsional moment, or torque. Thus, torsional shear stress is developed in the shaft. Also, a shaft usually carries power-transmitting component which is bevel gear, which exert forces on the shaft in the transverse direction (perpendicular to its axis). These transverse forces cause bending moments to be developed in the shaft, requiring analysis of the stress due to bending. In fact, these shafts must be analyzed for combined stress because of the simultaneous occurrence of torsional shear stresses and normal stresses due to bending.

$N = 1000rpm$

$F_t = 2149.8N$

The material used for shaft selected depending on the following criteria:

- It should have high strength
- It should have good machinability
- It should have low notch sensitivity factor
- It should have good it treatment properties
- It should have high wear resistance properties

So

$\sigma_{ut} = 540MPa$

$\sigma_y = 270MPa$

Table 14: Mechanical properties of shaft material

Steel	σ_{ut}	σ_y
Hot rolled structure steel,	410Mpa	250MPa
Grade 250 to As3679,		
Common shafting materials		
Bright steel As 1443		
Black steel As 1442		
-CS1020	400MPa	200MPa
-CS 1030	500MPa	250MPa
-CS 1040	540MPa	270MPa

* Source: (G. Richard et el, 2008)

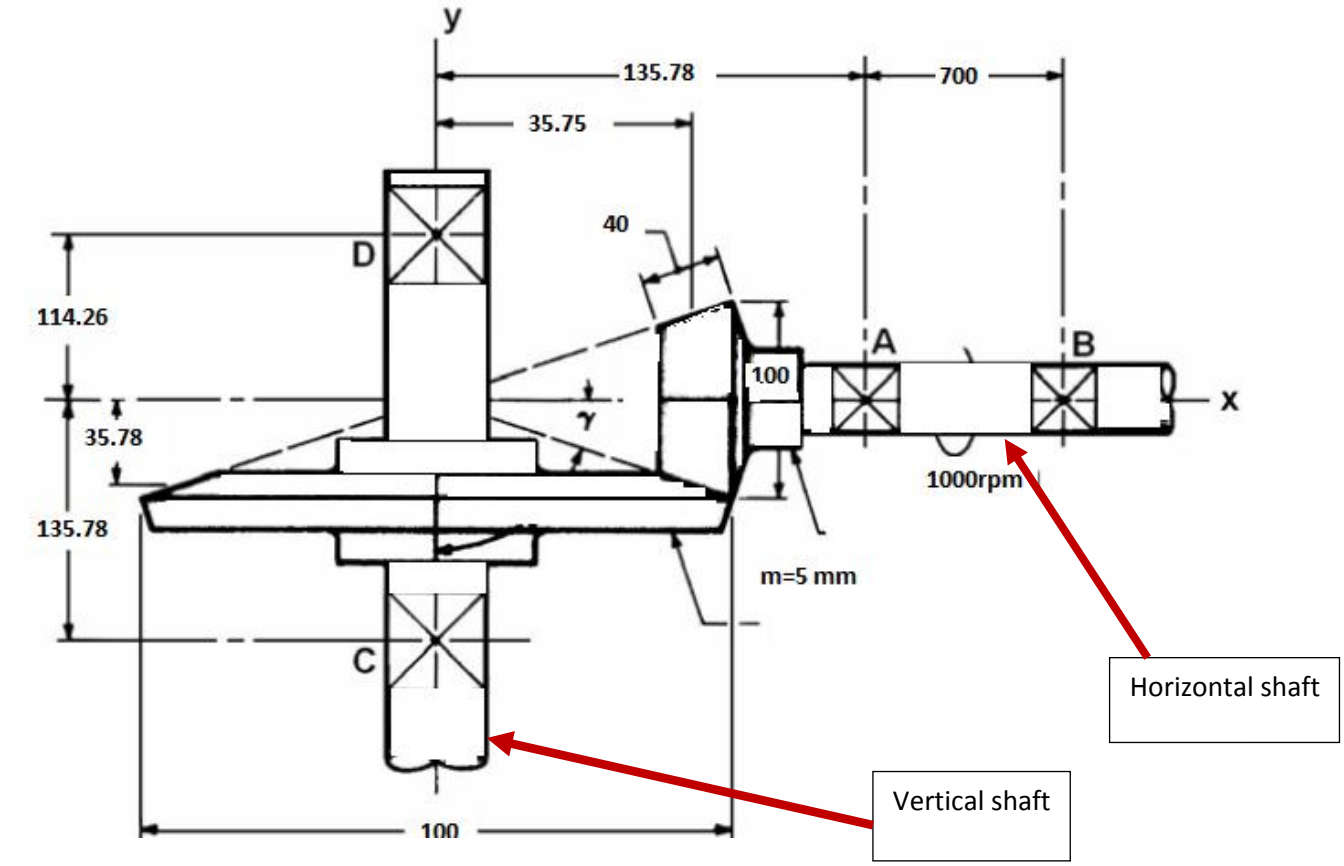

Figure 26: Bevel gear and shaft arrangement

In this case two force acting on shaft due to a mounting bevel gear

$F_r = F_t \tan \emptyset \cos \gamma_1$ (Eq.5.19)

$F_a = F_t \tan \emptyset \cos \gamma_2$ (Eq.5.20)

Where

F_r is radial force acting on shaft

F_a is axial force acting on shaft

$\emptyset = 20°$is pressure angle

$\gamma_1 = \gamma_2 = 45°$

By substituting the above value

$F_a = 2149.8 \times \tan 20° \cos 45°$

$F_a = 553\ N$

$F_r = 2149.8 \times \tan 20° \cos 45°$

$F_r = 553\ N$

$d2_{av} = d_2 - b \sin \gamma$ (Eq.5.21)

$d2_{av} = 100 - 40 \sin 45$

$d2_{av} = 71.71\ mm$

$d1_{av} = d_1 - b \sin \gamma$ (Eq. 5.22)

$d1_{av} = 100 - 40 \sin 45$

$d2_{av} = 71.71\ mm$

Vertical shaft analysis

Where F_t is acting in the x direction and F_a is in the y direction. All forces are acting at a distance of 38.8 mm from the shaft center line and 38.8 mm from the apex of the pitch cones as in Fig.27

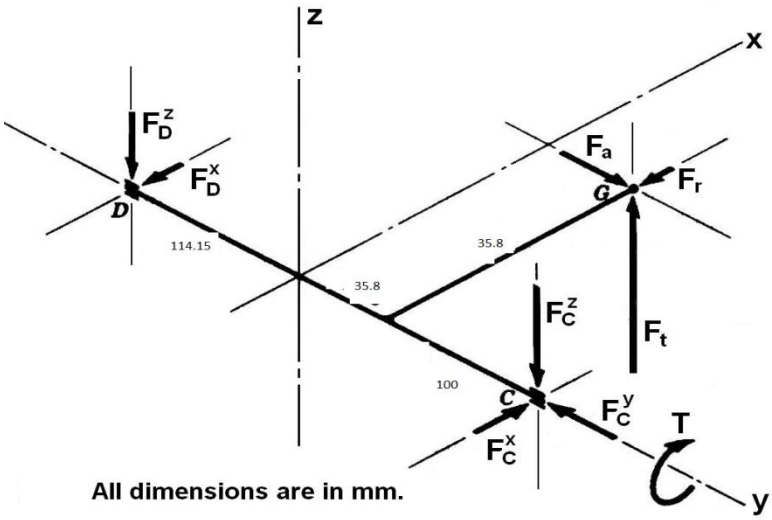

Figure 27: General Geometry of vertical shaft arrangement

Torque $T = F_t \times r2_{av}$

$T = 2149.8 \times 0.0358$

$T = 76.92\ N$

It is assumed that the bearing at point C takes the entire trust load, Hence

$F_C^y = F_a$

$F_C^y = 553\ N$

Taking moment about the horizontal axis through D

$\sum M_D = 0$ Because at point D the shaft is supported by bearing

$-F_C^Z \times 0.25 + F_t \times 0.15 = 0$

$-F_C^Z \times 0.25 + 2149.8 \times 0.15 = 0$

$F_C^Z = 1289.8\ N$

$\sum F_Z = 0$

$F_D^Z = 2149.8 - 1289.88$

$F_D^Z = 859.92$

Taking moment about the vertical axis through D

$\sum Mv_D = 0$

$F_C^X \times 0.25 - F_r \times 0.15 - F_a \times 0.0358 = 0$

$F_C^X \times 0.25 - 553 \times 0.15 - 553 \times 0.0358 = 0$

$F_C^X = 411.14\ N$

Taking moment about the vertical axis through C

$\sum Mv_C = 0$

$F_D^X \times 0.25 + F_r \times 0.15 - F_a \times 0.0358 = 0$

$F_D^X \times 0.25 + 553 \times 0.15 - 553 \times 0.0358 = 0$

$F_D^X = -252.49\ N$

The maximum bending moment occurs at point where bevel gear is mounted

Bending moment in case of x-y plane

$M_{Gxy} = F_D^x \times 0.15 - F_a \times 0.0358$

$M_{Gxy} = -252.44 \times 0.15 - 553 \times 0.0358$

$M_{Gxy} = 57.678\ Nm$

Bending moment in case of x-z plane

$M_{Gxz} = F_D^Z \times 0.15 - F_t \times 0.0358$

$M_{Gxz} = 859.19 \times 0.15 - 2149.8 \times 0.0358$

$M_{Gxz} = 53.635\ Nm$

The total bending at point G

$M_G = \sqrt{M_{Gxy}^2 + M_{Gxy}^2}$

$M_G = \sqrt{57.678^2 + 53.635^2}$

$M_G = 78.76\ Nm$

The shaft daimeter using DE-Goodman cirterian

$$d = \left[\frac{16n}{\pi}\left(\frac{2\left(k_f M_G\right)}{\sigma_e} + \frac{\left[3\left(k_{sf}T\right)^2\right]^{1/2}}{\sigma_{ut}}\right)\right]^{1/3} \qquad \text{(Eq. 5.23)}$$

From table estimate $k_f = 1.7$, $k_{sf} = 1.5$ crossebonding to rotating shaft under suddenly applied load with minor shocks only

Table 15: Recommended value of K_{sf} and K_t

Nature of load	K_{sf}	K_f
1. Stationary shafts		
a. Gradually applied load	1.0	1.0
b. Suddenly applied load	1.5 to 2.0	1.5 to 2.0
2. Rotating shafts		
a. Gradually applied or steady load	1.5	1.0
b. Suddenly applied load with minor shocks only	1.5 to 2.0	1.5 to 2.0
c. Suddenly applied load with heavy shocks	2.0 to 3.0	1.5 to 3.0

* Source: (Richard et al, 2008)

Assume $, n = 1.5$ and $k_r = 0.81$ from table corrosbonding to 0.99 relabilty

Table 16: Reliability factor

Desired reliability (%)	Reliability factor
0.5	1
0.9	0.9
0.99	0.81
0.999	0.75

* Source: (Richard et al, 2008)

$k_c = k_d = k_e = 1$

$\sigma_e' = 0.5\sigma_{ut}$ for $\sigma_{ut} \leq 1400\ Mpa$

$\sigma_e = k_a k_r k_c k_d k_e k_f 0.5\sigma_{ut}$ (Eq.5.24)

$k_a = a\sigma_{ut}^b$ (Eq.5.25)

The value of a and b from table crossponding to hot- rolled surface finish

Table 17: Parameters for Marin Surface Modification Factor

Surface finish	Factor (a)	Exponent
Ground	1.58	-0.085
Machined or cold-draw	4.51	-0.265
Hot-rolled	57.7	-0.718
As-forged	27.2	-0.995

* Source: Source: (Richard et al, 2008)

$a = 57.7$

$b = -0.718$

$k_a = 57.7 \times 540^{-0.718}$

$k_a = 0.629$

$\sigma_e = 0.629 \times 0.81 \times 0.5 \times 540$

$\sigma_e = 137.56\ Mpa$

$$d = \left[\frac{16 \times 1.5}{\pi}\left(\frac{2(1.7 \times 78.76)}{137.56\ Mpa} + \frac{[3(1.5 \times 76.92)^2]^{1/2}}{540\ Mpa}\right)\right]^{1/3}$$

$d = 26.06\ mm$

Taking of the standard shaft

$d = 30\ mm$

To check the shaft is safe or not we use

$$\left(\frac{\sigma}{\sigma_e'}\right)^2 + \left(\frac{\tau}{\sigma_y}\right)^2 = 1$$ (Eq.5.27)

Where $\sigma\ and\ \tau$ at the critical point in our case the critical point is C

$$\sigma = \frac{32M_e}{\pi d^3} = \frac{32 \times 78.26}{\pi \times 0.03^3} = 45.37\ Mpa$$

$$\tau = \frac{16T_e}{\pi d^3} = \frac{16 \times 76.92}{\pi \times 0.03^3} = 22.30\ Mpa$$

Therefore

$$\left(\frac{45.37}{137.56}\right)^2 + \left(\frac{22.30}{270}\right)^2 \leq 1$$

$0.0068 \leq 1$

So the vertical shaft safe under this load

Horizontal shaft

These shafts transmit power from the tractor to the gear of teff spreading machine. It is made of the same material as the vertical shaft and we made assumption at point A and C (bearing) it has the capacity to resist axial load

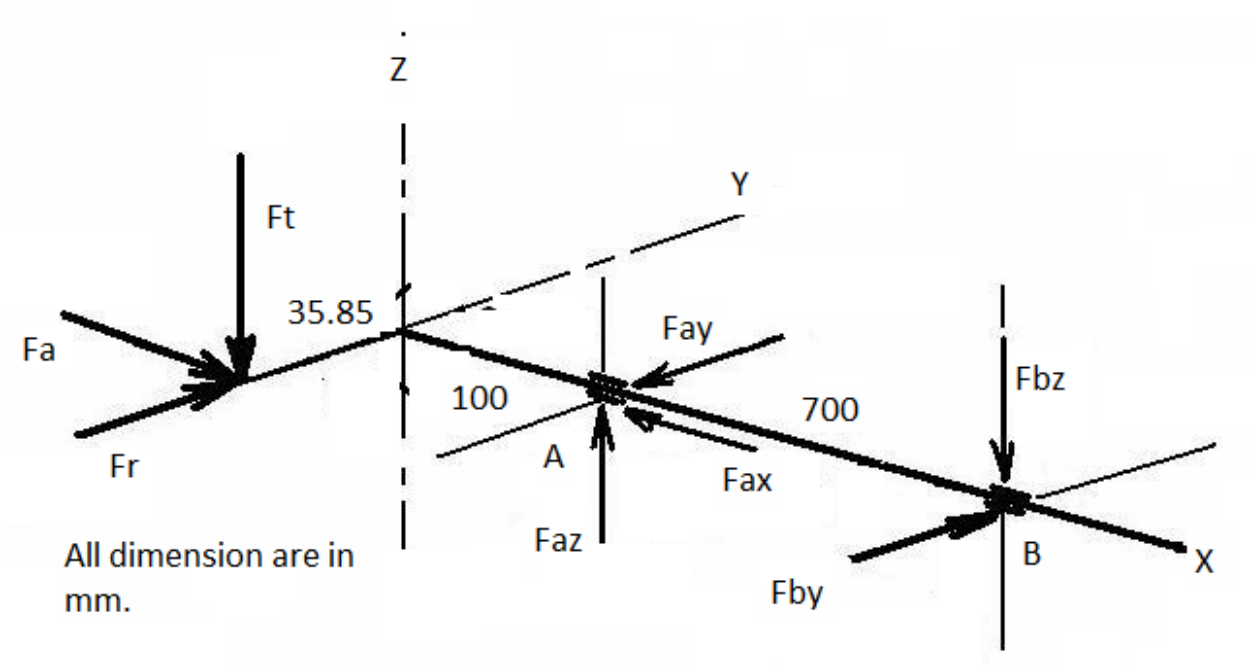

Figure 28: General geometry of horizontal shaft

Torque $T = F_t \times 1$

$T = 2149.8 \times 0.0358$

$T = 76.92\ N$

It is assumed that the bearing at point A takes the entire trust load, Hence

$F_A^x = F_a$

$F_A^x = 553\ N$

Taking moment about the horizontal axis through B

$\sum M_B = 0$ Because at point D the shaft is supported by bearing

$-F_A^Z \times 0.7 + F_t \times 0.8 = 0$

$-F_A^Z \times 0.7 + 2149.8 \times 0.8 = 0$

$F_A^Z = -2456.9\ N$

$\sum F_Z = 0$

$F_B^Z = 2149.8 - 2456.9$

$F_B^Z = -307.11\ N$

Taking moment about the vertical axis through B

$\sum Mv_B = 0$

$F_A^y \times 0.7 - F_r \times 0.8 - F_a \times 0.0358 = 0$

$F_A^y \times 0.7 - 553 \times 0.8 - 553 \times 0.0358 = 0$

$F_A^y = 603.718\ N$

$\sum F_y = 0$

$F_B^y = 603.18 - 553$

$F_B^y = 50.718\ N$

The maximum bending moment occurs at point where bevel gear is mounted

Bending moment in case of x-y plane

$M_{Gxy} = F_a \times 0.0358$

$M_{Gxy} = 553 \times 0.0358$

$M_{Gxy} = 19.79\ Nm$

Bending moment in case of x-z plane

$M_{Gxz} = F_t \times 0.0358$

$M_{Gxz} = 2149.8 \times 0.0358$

$M_{Gxz} = 77.07\ Nm$

The total bending at point G

$$M_G = \sqrt{M_{Gxy}^2 + M_{Gxy}^2} \qquad \text{(Eq.5.28)}$$

$M_G = \sqrt{19.79^2 + 77.07^2}$

$M_G = 79.57\ Nm$

The shaft daimeter using DE-Goodman cirterian

$$d = \left[\frac{16n}{\pi}\left(\frac{2\left(k_f M_G\right)}{\sigma_e} + \frac{\left[3\left(k_{sf}T\right)^2\right]^{1/2}}{\sigma_{ut}}\right)\right]^{1/3}$$

From table estimate $k_f = 1.7$, $k_{sf} = 1.5$ crossebonding to rotating shaft under suddenly applied load with minor shocks only

Assume , $n = 1.5$ and $k_r = 0.81$ from table corrosbonding to 0.99 relabilty

$k_c = k_d = k_e = 1$

$\sigma_e' = 0.5\sigma_{ut}$ for $\sigma_{ut} \leq 1400\ Mpa$

$\sigma_e = k_a k_r k_c k_d k_e k_f 0.5\sigma_{ut}$

$k_a = a\sigma_{ut}^b$

The value of a and b from table crossponding to hot- rolled surface finish

$a = 57.7$

$b = -0.718$

$k_a = 57.7 \times 540^{-0.718}$

$k_a = 0.629$

$\sigma_e = 0.629 \times 0.81 \times 0.5 \times 540$

$\sigma_e = 137.56\ Mpa$

$$d = \left[\frac{16 \times 1.5}{\pi}\left(\frac{2(1.7 \times 79.56)}{137.56\ Mpa} + \frac{[3(1.5 \times 77.07)^2]^{1/2}}{540\ Mpa}\right)\right]^{1/3}$$

$d = 26.06\ mm$

Takeing the standard shaft

$d = 30\ mm$

To check the shaft is safe or not we use Goodman criteria

$$\left(\frac{\sigma}{\sigma_e{}'}\right)^2 + \left(\frac{\tau}{\sigma_y}\right)^2 = 1$$

Where $\sigma\ and\ \tau$ at the critical point in our case the critical point is C

$$\sigma = \frac{32M_e}{\pi d^3} = \frac{32 \times 79.56}{\pi \times 0.03^3} = 45.37\ Mpa$$

$$\tau = \frac{16T_e}{\pi d^3} = \frac{16 \times 77.92}{\pi \times 0.03^3} = 22.30\ Mpa$$

Therefore

$$\left(\frac{45.37}{137.56}\right)^2 + \left(\frac{22.30}{270}\right)^2 \leq 1$$

$0.0068 \leq 1$, so the vertical shaft safe under this load

5.6. Key design

The diameters of the shafts are 30mm.

Standard table crossbonding to shaft diameters

Width of key (w) = 8 mm

Height of key (w) = 3.3 mm

Assuming, material the shaft to be AISI 1035 CD Steel which has a shear stress of 46 MPa.

The length of key(L) is obtained by considering the key in shearing and crushing

Considering shearing of the key. We know that shearing strength (or torque transmitted) of the key

$$T = L \times w \times \tau \times \frac{D}{2} \qquad \text{(Eq. 5.29)}$$

$$T = L \times 8\,mm \times 46 \times \frac{30}{2} = 5520L$$

Torsional shearing strength (or torque transmitted) of the shaft to be

$$T = \frac{\pi}{16} \times \sigma \times d^3 \qquad \text{(Eq. 5.30)}$$

$$T = \frac{\pi}{16} \times 46 \times 30^3 = 243742.5\,Nmm$$

By equating two equation

$$5520L = 243742.5$$

$$L = 44.15\,mm$$

5.7. Bearing selection

Bearing must be selected based on its load carrying capacity, life expectancy and reliability (PSG Tech 1989).

For vertical shaft,

The reaction forces in the radial and in the axial direction at bearing A

$F_A^x = F_a = 553\ N$

$F_A^y = 603.718\ N$

$F_A^z = 2456.9\ N$

$F_r = \sqrt{F_A^{y\,2} + F_A^{z\,2}}$

$F_r = \sqrt{2456.9^2 + 603.718^2}$

$F_r = 2529.98\ N$

The rotational speed of the shaft

$N = 1000rpm$

It is assumed that the bearing works 8hours per day and changed for every 5years

$T = 5years \times 10hours\ per\ days \times 313days\ per\ years$

$T = 15650hours$

Then the life of the bearing is

$L_d = T \times N \times 60$ (Eq. 5.31)

$L_d = 15650 \times 1000 \times 60$

$L_d = 939 \times 10^6 revolution$

Then basic dynamic equivalent radial load is

$W_d = F_r XV + YF_a$ (Eq.5.32)

Where

X is radial load factor and equal to 0.56

Y is axial load factor and from table 3.4 taking the average 1.5

V=1 for inner races rotates

Table 18: Axial load factor

F_a/C_s	0.014	0.028	0.058	0.084	0.11	0.17	0.28	0.42	0.56
Y	2.3	1.99	1.71	1.55	1.45	1.31	1.55	1.04	1.0

*Source: (Richard et al, 2008)

$W_d = 0.56 \times 1 \times 2529.98\ N + 1.5 \times 553\ N$

$W_d = 2146.29\ N$

Then the basic dynamics load rating is

$C_d = W_d \left(\frac{L_d}{L_s}\right)^{1/K}$ (Eq. 5.33)

Where

K=3 for ball bearing

L_S=10^6 revolution

$C_d = 2146.29\ N \times \left(\frac{939 \times 10^6}{10^6}\right)^{1/3}$

$C_d = 20.12\ KN$

From standard table (Mechanical design, shigly 9th edition) we selected corresponding to the angular contact ball bearing

$$C_s = 11\ KN\ \ and\ \ C_d = 20.3\ KN$$

Table 19: Selected Angular contact ball bearing at point A

D_B	D_O	width	C_{10}	C_0
30	72	17	20.3 KN	11 KN

Then to verify the assumption

$$F_a/C_s = \frac{553}{11000} = 0.0502$$

Then from table 18 the axial load factor is 1.701 by interpolating

Then the adjusted basic dynamic radial load is

$$W_d = 0.56 \times 1 \times 2156.9 + 1.701 \times 553$$

$$W_d = 2148.56\ N$$

The adjusted basic dynamic load rating is

$$C_d = 2148.56\left(\frac{939\times10^6}{10^6}\right)^{1/3}$$

$$C_d = 20.001\ KN$$

The adjusted dynamic load rating is less than the selected bearing dynamic load rating so the selected bearing meets the design criteria.

For second bearing at point B the reaction forces in the radial:

$$F_B^Y = 50.718\ N$$

$$F_Z^Y = 307.11\ N$$

$$F_r = \sqrt{50.78^2 + 307.11^2}$$

$$F_r = 311.27\ N$$

Then the basic dynamics load rating is

$$C_d = F_r \left(\frac{L_d}{L_s}\right)^{1/K}$$

Where

K=3 for ball bearing

$L_s = 10^6$ revolution

$$C_d = 311.27 \times \left(\frac{939 \times 10^6}{10^6}\right)^{1/3}$$

$$C_d = 3.048\ KN$$

From standard table (Mechanical design, shigly 9th edition) we selected 306 single row angular ball bearings

Table 20: Selected Angular contact ball bearing at point B

	D_B	D_O	Width	Balls Dia.	No.	C_{10}
306	30 mm	72 mm	19 mm	$\frac{3}{8}\frac{1}{4}$	9	3360 N

For horizontal shaft

The reaction forces in the radial and in the axial direction at bearing C

$$F_C^Y = F_a = 553\ N$$

$$F_C^x = 411.14\ N$$

$$F_C^z = 1289.8\ N$$

$$F_r = \sqrt{F_C^{X\,2} + F_C^{z\,2}}$$

$F_r = \sqrt{1289.8^2 + 411.14^2}$

$F_r = 1353.8\ N$

The rotational speed of the shaft

$N = 1000rpm$

It is assumed that the bearing works 8hours per day and changed for every 5years

$T = 5years \times 10hours\ per\ days \times 313days\ per\ years$

$T = 15650hours$

Then the life of the bearing is

$L_d = T \times N \times 60$ (Eq. 5.34)

$L_d = 15650 \times 1000 \times 60$

$L_d = 939 \times 10^6 revolution$

Then basic dynamic equivalent radial load is

$W_d = F_r XV + YF_a$ (Eq.5.35)

Where

X is radial load factor and equal to 0.56

Y is axial load factor and from table 11 taking the average 1.5

V=1 for inner races rotates

$W_d = 0.56 \times 1 \times 1353.83\ N + 1.5 \times 553\ N$

$W_d = 1587.64N$

Then the basic dynamics load rating is

$$C_d = W_d \left(\frac{L_d}{L_s}\right)^{1/K} \quad \text{(Eq. 5.36)}$$

Where

K=3 for ball bearing

L_S= 10^6 revolution

$$C_d = 1587.64\ N \times \left(\frac{939 \times 10^6}{10^6}\right)^{1/3}$$

$$C_d = 18.52\ KN$$

From standard table (Mechanical design, shigly 9th edition) we selected corresponding to the angular contact ball bearing

$$C_s = 11\ KN \ \ and \ \ C_d = 20.3KN$$

Table 21: Selected Angular ball bearing at point C

D_B	D_O	width	C_{10}	C_0
30	62	16	20.3 KN	11KN

Then to verify the assumption

$$F_a/C_s = \frac{553}{11000} = 0.0502$$

Then from table 18 the axial load factor is 1.728 by interpolating

Then the adjusted basic dynamic radial load is

$$W_d = 0.56 \times 1 \times 1587.64 + 1.728 \times 553$$

$$W_d = 1845.03\ N$$

The adjusted basic dynamic load rating is

$$C_d = 1845.03\left(\frac{939 \times 10^6}{10^6}\right)^{1/3}$$

$$C_d = 18.067\ KN$$

The adjusted dynamic load rating is less than the selected bearing dynamic load rating so the selected bearing meets the design criteria.

For second bearing at point D the reaction forces in the radial:

$$F_D^X = 859.92\ N$$

$$F_D^X = 252.49\ N$$

$$F_r = \sqrt{859.92^2 + 252.49^2}$$

$$F_r = 898.21\ N$$

Then the basic dynamics load rating is

$$C_d = F_r\left(\frac{L_d}{L_s}\right)^{1/K}$$

Where

K=3 for ball bearing

$$L_s = 10^6 \quad revolution$$

$$C_d = 898.21 \times \left(\frac{939 \times 10^6}{10^6}\right)^{1/3}$$

$$C_d = 8.79\ KN$$

From standard table (Mechanical design, shigly 9th edition) we select single row 02-series angular ball bearing

Table 22: Selected angular ball bearing at point D

	D_B	D_O	Width	Balls Dia.	C10	C_0
306	30 mm	62mm	16 mm	$\frac{3}{8}\frac{1}{4}$	20.3KN	11 K N

6. Cost analysis

Table 23 shows that the cost of each component of spinning disc *teff* seed broadcaster and the overall cost of the machine.

Table 23: Total cost

No	Item	Unit	Quantity	Unit cost	Total cost
1	Mild steel flat sheet metal thickness 3-5 mm	Seq meter	4	800	3200 Birr
2	Black Carbone steel CS 1042	Meter	3	400	1200 Birr
3	Ball Bearing	Pcs	4	150	600 Birr
4	Bevel gear	pcs	2	3500	7000 Birr
5	Circular Iron	Meter	5	100	500 Birr
6	Bolt and nut	Pcs	16	10	160 Birr
7	Rivet	Pcs	16	5	80 Birr
8	Keys	Pcs	4	50	200 Birr
	Overall cost				**12940 Birr**

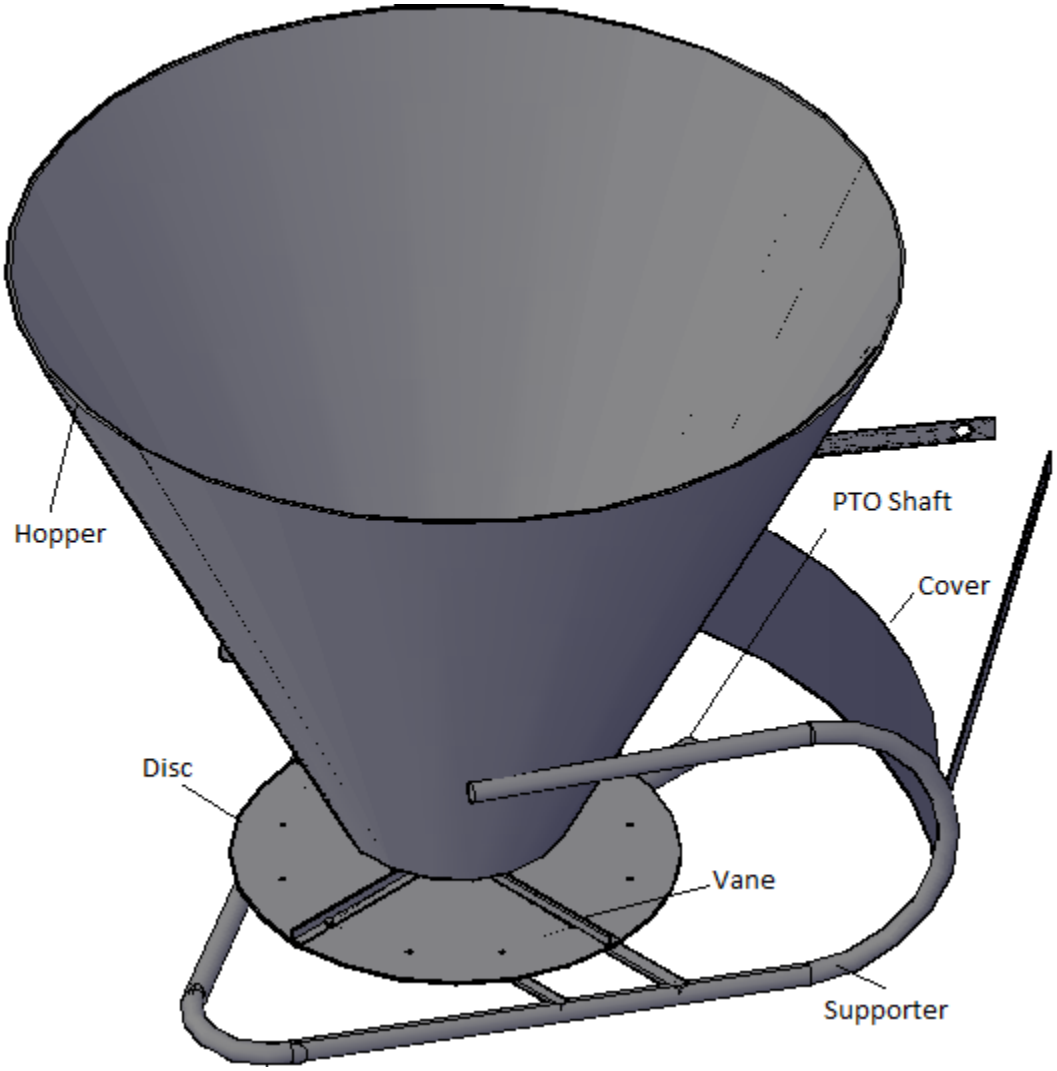

Figure 29: Assembly of *Teff* seed broadcaster

7. Conclusion

- Based on the collected date from literature, gathering of information from research organization, developing of mathematical model for a single *teff* seed on-disc and off-disc, and design of different machine parts, a *teff* seed broadcasting machine has been analyzed and designed.
- Based on the physical properties of *teff* seed, as the coefficients of friction of *teff* seed changes from 0.29 to 0.53 corresponding to changing of the point where the *teff* seed leave the disc and also change the projected distance of *teff* seed.
- Based on the machine parameters, the projected distance of *teff* seed as well as the point where *teff* seed leave the disc was changed due to change of the cone angle, the pitch angle and the rotational speed of disc.
- This study have investigated the mass flow rate of *teff* seed and the size of hopper which has the capacity to hold 90 kg of teff seed
- This study set out the minimum diameters of two shafts, the diameter of shaft is 30 mm under bending and torsion moment and checked stability of shaft using Goodman equation criteria and was found safe.
- There was also determining the size of 90^0 mounting bevel gears and it has 5 mm module, 40 mm width and 100 mm diameter and checked for their contact and fatigue stress on tooth and were found within the allowable limits in the maximum load condition.
- It also selects four bearings, which have bore diameter 30mm and two of these bearings have ability to resist axial loads.
- It is recommended that the machine should be developed and tested in laboratory and filed test to examine the result with numerical solution.

Reference

Aphale, A., N. Bolander, J. Park, L. Shaw, J. Svek and C. Wassgren (2003). Granular fertiliser particle dynamics on and off a spinner spreader. *Biosystems Engineering*, 85(3): 319-329

Ball, B. C. (1986). Cereal production with broadcast seed and reduced tillage: a review of recent experimental and farming experience. *J. Agri. Eng. Res*. 35(2), 71-95

Hofstee, J.W. (1995). Handling and spreading of fertilisers: Part 5, the spinning disc type fertiliser spreader. *J. Agric. Engng. Res.* 62: 143-162

Ileleji K.E and Zhou.B. (2008). The angle of repose of bulk corn Stover particles. Powder technology. 187:110-118

Mufalubi.A.A. (2007). Development of Rice polishing Machine; AU J.T.11(2):105-112

M.F.Spotts. Design of machine elements. Third edition. Prentic-Hall, USA

Patterson and Reece (1962). Motion of spherical particles on a spinner disc; American Society of Agricultural Engineers; Vol. 47(5): 1389−1404

Seyfu, K (1997). Teff(Eragrostis teff (Zucc.)Trotter). Promoting the Conservation and Use of Under-Utilised Neglected Crops, 12, IPGRI, Italy

R.S. Kmurmi and J.K.Gupta (2005). A text book of machine design. S.I.(Meteric) ed. Ram Nagar, New Delhi

Shigley. J.E (2011). Mechanical Engineering Design. Nine edition. McGraw-Hill. Newyork, USA

Tajuddin, A. 1989. Design development and testing of hand rotary broadcasting device for seeds, fertilizers and granular insecticides. Agricultural Mechanization in Asia, Africa

and Latin-America (AMA) 20(1): 41-44.

Ziauddin, A.T.M. and P. Roy. 1997. Design and Development of a seed-cum-fertilizer distributor for small farm holders. Journal of the Institution of Engineers, Bangladesh. Vol. 25/AE (1):60-67.

Zewdu, A D and W. K. Solomon (2007). Moisture-dependent physical properties of teff seed, *Biosystems Engineering*, 96(1): 57-63 doi: 10.1016/j. Biosystemseng. 2006.09.008

Appendix

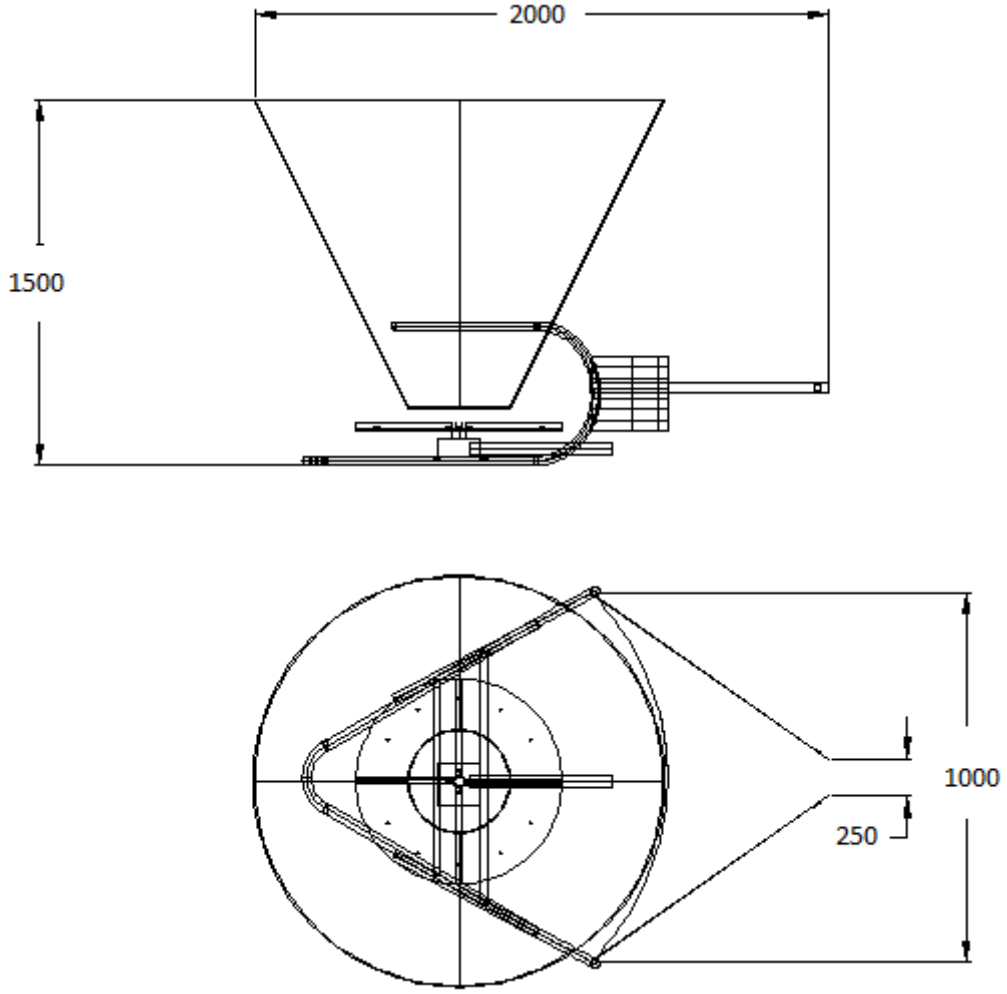

Drawn by	Abdulhakim Shukurea		Drawing Number	01
Approved by	Zewdu Abdi (Dr.-Ing)		Date	31/10/2012
Title	Assembly		Approved Date	2/11/2012
Material			Scale	1:10
Dimensions	mm		Sheet number	01
AAIT				

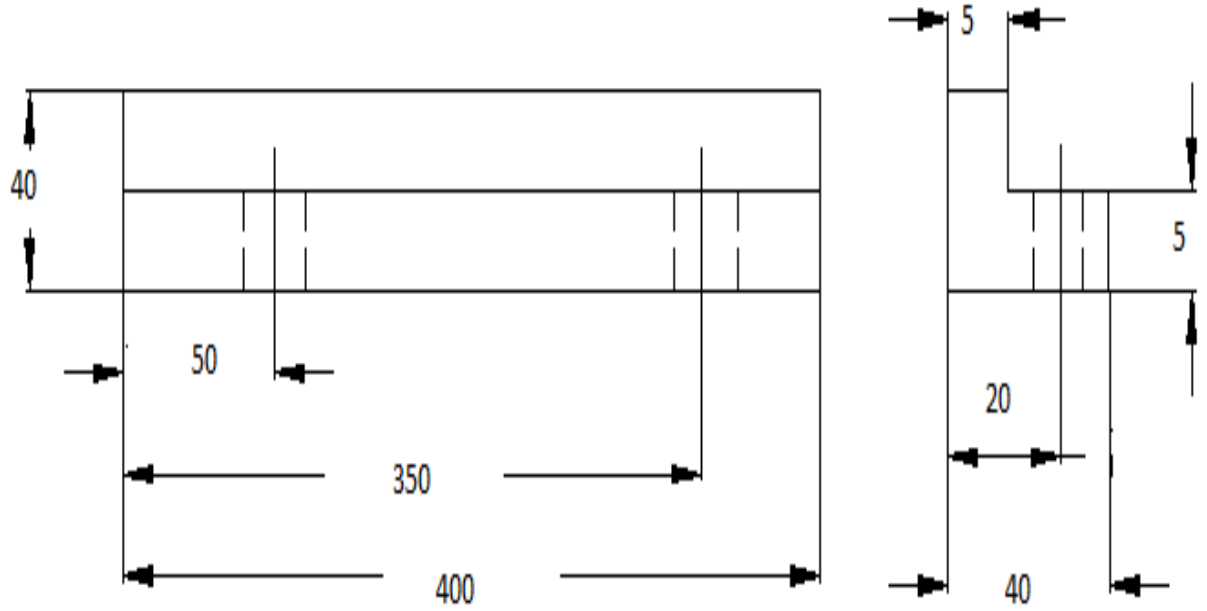

Drawn by	Abdulhakim Shukurea		Drawing Number	02
Approved by	Zewdu Abdi (Dr.-Ing)		Date	31/10/2012
Title	Vane		Approved Date	2/11/2012
Material	Mild steel flat sheet		Scale	1:5
Quantity	4		Sheet number	02
Dimensions	mm			

AAIT

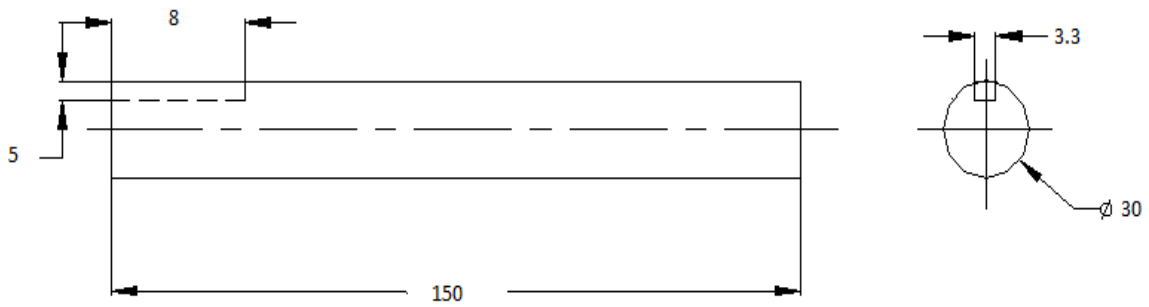

Drawn by	Abdulhakim Shukurea		Drawing Number	03
Approved by	Zewdu Abdi (Dr.-Ing)		Date	31/10/2012
Title	Shaft		Approved Date	2/11/2012
Material	Black steel As 1442 CS 1042		Scale	1:5
Quantity	1		Sheet number	03
Dimensions	mm			

AAIT

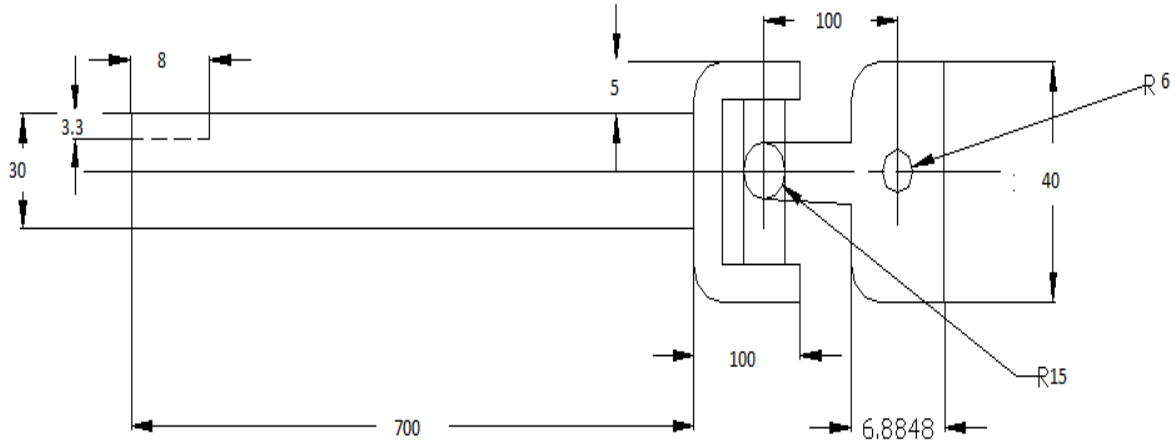

Drawn by	Abdulhakim Shukurea		Drawing Number	04
Approved by	Zewdu Abdi (Dr.-Ing)		Date	31/10/2012
Title	Pto Shaft		Approved Date	2/11/2012
Material	Black steel As 1442 CS 1042		Scale	1:5
Quantity	1		Sheet number	04
Dimensions	mm			

AAIT

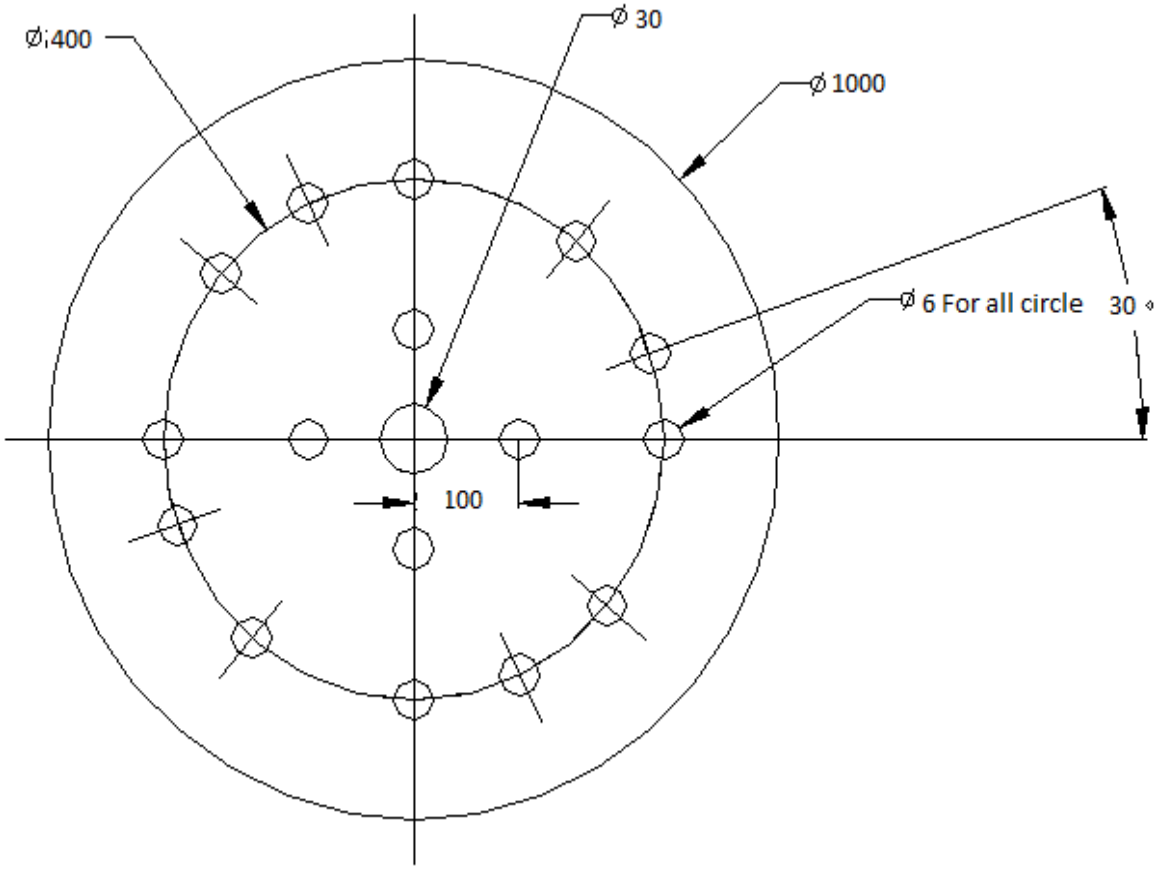

Drawn by	Abdulhakim Shukurea		Drawing Number	05
Approved by	Zewdu Abdi (Dr.-Ing)		Date	31/10/2012
Title	Spinning Disc		Approved Date	2/11/2012
Material	Mild steel flat sheet		Scale	1:5
Dimensions	mm		Sheet number	05

AAIT

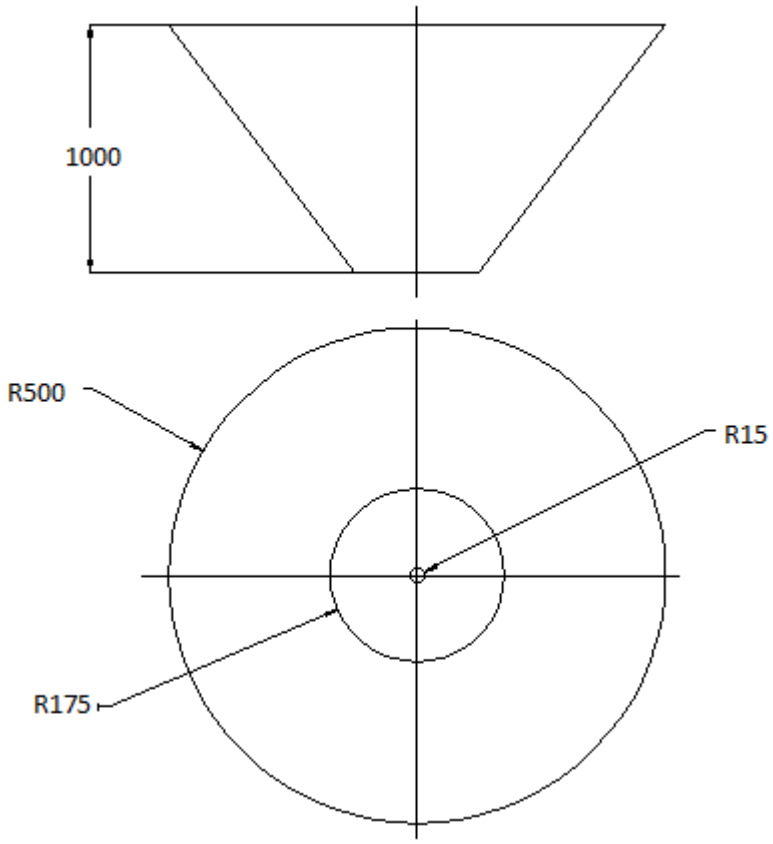

Drawn by	Abdulhakim Shukurea		Drawing Number	06
Approved by	Zewdu Abdi (Dr.-Ing)		Date	31/10/2012
Title	Vane		Approved Date	2/11/2012
Material	Mild steel flat sheet		Scale	1:5
Quantity	4		Sheet number	06
Dimensions	mm			

AAIT